

## Exact $g$ -function flows from the staircase model

Patrick Dorey<sup>1</sup>, Roberto Tateo<sup>2</sup> and Ruth Wilbourne<sup>1</sup>

<sup>1</sup>*Department of Mathematical Sciences, Durham University,  
South Road, Durham DH1 3LE, UK*

<sup>2</sup>*Dip. di Fisica Teorica and INFN, Università di Torino,  
Via P. Giuria 1, 10125 Torino, Italy*

p.e.dorey@durham.ac.uk, tateo@to.infn.it,  
r.m.wilbourne@durham.ac.uk

### Abstract

Equations are found for exact  $g$ -functions corresponding to integrable bulk and boundary flows between successive unitary  $c < 1$  minimal conformal field theories in two dimensions, confirming and extending previous perturbative results. These equations are obtained via an embedding of the flows into a boundary version of Al. Zamolodchikov's staircase model.

# 1 Introduction

The exact  $g$ -function [1,2] is a powerful tool for the study of integrable boundary flows, allowing the results of, for example, [3,4] to be extended to situations where the bulk is not critical. The initial proposals of [1] were restricted to cases where the bulk theory possessed only massive excitations, and their scattering was diagonal both in the bulk and at the boundary. Recently, in [5], equations were introduced to describe the exact  $g$ -function for the simplest case where massless bulk degrees of freedom persist even in the far infrared, namely the flow between the tricritical and critical Ising models. As mentioned in [5], these ‘massless’  $g$ -function flow equations can be obtained from a consideration of the so-called staircase models, and as a result are naturally embedded in a much richer set of flows linking the boundary behaviours of all of the unitary  $c < 1$  minimal models of conformal field theory. In this paper we will provide some more details of this larger pattern, and in the process propose equations to describe  $g$ -function flows between all neighbouring pairs of unitary minimal models. For all of these cases beyond the first (which is the already-discussed flow between tricritical and critical Ising models), bulk scattering is non-diagonal. However, the  $g$ -function equations have a simple form which naturally generalises previously-seen structures<sup>1</sup>.

The staircase connection naturally leads us to equations which describe two-parameter families of boundary perturbations, special cases of which match the one-parameter flows found perturbatively in [9], and which therefore also match the results for fluctuating geometries found in [10]. We expect that our more-general sets of flows from superpositions of boundary states can be generalised yet further, to describe integrable bulk and boundary deformations of boundary conformal field theories with arbitrary numbers of boundary parameters. At the level of the exact  $g$ -function equations the generalisation is rather clear, and will be indicated below. However we will leave the detailed investigation of this point for further work, as the two-parameter situation is already quite involved.

## 2 The staircase model, in the bulk and at the boundary

The staircase model was originally introduced by Al.B.Zamolodchikov in [11]; various generalisations can be found in [12–15]. Its S-matrix encodes the diagonal scattering of a single massive particle of mass  $M$ , and can be obtained by the analytic continuation of the S-matrix of the sinh-Gordon model to those complex values of the coupling constant where real-analyticity holds. At the level of the Lagrangian the meaning of this continuation remains somewhat obscure, but as an S-matrix theory the model appears to make perfect sense, and leads to a consistent picture of finite-size effects described exactly by thermodynamic Bethe ansatz (TBA) equations which are derived in the standard way from the S-matrix. Trading the analytically-continued sinh-Gordon coupling for a real parameter  $\theta_0$ , the staircase S-matrix is

$$S(\theta) = \tanh\left(\frac{\theta-\theta_0}{2} - \frac{i\pi}{4}\right) \tanh\left(\frac{\theta+\theta_0}{2} - \frac{i\pi}{4}\right) \quad (2.1)$$

and this leads to the following TBA equations for the pseudoenergy  $\epsilon(\theta)$  for the system on a circle of circumference  $R$ :

$$\epsilon(\theta) = r \cosh \theta - \int_{\mathbb{R}} \phi_S(\theta - \theta') L(\theta') d\theta' \quad (2.2)$$

---

<sup>1</sup>As we were writing this paper, an alternative derivation of the diagonal  $g$ -function flow equations of [1,2,5], was presented, in [6] (see also [7]). It will be worthwhile, and appears in most respects to be straightforward, to generalise the approach of [6] to cover our new equations, but as we feel the staircase aspect is of independent interest we have decided to leave this point for the time being. We should also mention that boundary  $g$ -functions in the staircase model were previously discussed, amongst other things, in [8], but since that paper predated the exact  $g$ -function results of [1], its conclusions for situations with off-critical bulk were not correct.

where  $r = MR$ , and

$$L(\theta) = \ln(1 + e^{-\epsilon(\theta)}), \quad \phi_S(\theta) = -\frac{i}{2\pi} \frac{d}{d\theta} \ln S(\theta). \quad (2.3)$$

The ground state energy of the system is then given by  $E(R) = -\frac{\pi}{6R} c_{\text{eff}}(r)$ , where the effective central charge  $c_{\text{eff}}(r)$  is

$$c_{\text{eff}}(r) = \frac{6}{\pi^2} \int_{\mathbb{R}} r \cosh(\theta) L(\theta) d\theta. \quad (2.4)$$

For later use we define

$$(x)(\theta) = \frac{\sinh\left(\frac{\theta}{2} + \frac{i\pi x}{2}\right)}{\sinh\left(\frac{\theta}{2} - \frac{i\pi x}{2}\right)}, \quad \phi_{(x)}(\theta) = -\frac{i}{2\pi} \frac{d}{d\theta} \ln (x)(\theta) = \frac{-\sin(\pi x)/(2\pi)}{\cosh(\theta) - \cos(\pi x)}, \quad (2.5)$$

and also

$$\phi(\theta) = -\phi_{(\frac{1}{2})}(\theta) = \frac{1}{2\pi \cosh(\theta)} \quad (2.6)$$

so that the staircase kernel  $\phi_S(\theta)$  is

$$\phi_S(\theta) = \phi(\theta - \theta_0) + \phi(\theta + \theta_0). \quad (2.7)$$

For large values of  $\theta_0$ , this function is localised about  $\theta = \pm\theta_0$ , as illustrated in figure 1.

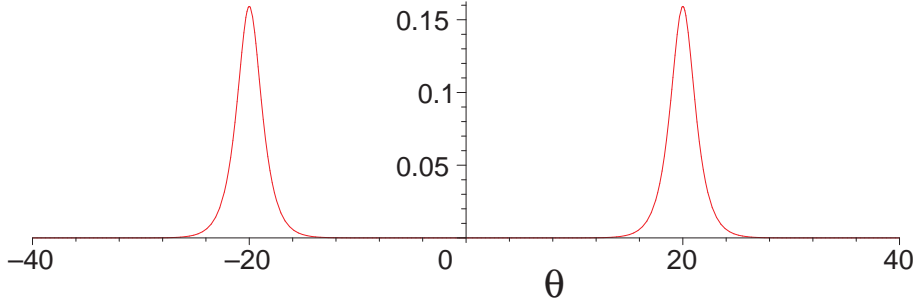


Figure 1: The staircase kernel  $\phi_S(\theta)$  for  $\theta_0 = 20$ .

The TBA system (2.2) therefore couples the values of the pseudoenergy  $\epsilon(\theta)$  near to  $\theta$  with those near to  $\theta \pm \theta_0$ , and the behaviour of the effective central charge  $c_{\text{eff}}(r)$  depends crucially on how many times the interval  $[0, \theta_0]$  fits into the range  $[-\ln(\frac{1}{r}), \ln(\frac{1}{r})]$ , beyond which the value of the pseudoenergy is dominated by the driving term  $r \cosh \theta$  in (2.2), irrespective of its coupling to values taken elsewhere. Referring the reader to [11, 13] for further explanation, the net result is that  $c_{\text{eff}}(r)$  develops a series of plateaux, or steps, which become more pronounced as  $\theta_0 \rightarrow \infty$ . (The top curves on figures 3a-3d below show  $c_{\text{eff}}(r)$  for  $\theta_0 = 60$ , by which point the plateaux are already quite sharply defined.) Indexing the steps by an integer  $m = 3, 4 \dots$ , the  $(m-2)^{\text{th}}$  step is found for  $-(m-2)\theta_0/2 \ll \ln(r) \ll -(m-3)\theta_0/2$ , and on this step,  $c_{\text{eff}}(r) \rightarrow c_m$  as  $\theta_0 \rightarrow \infty$ , where

$$c_m = 1 - \frac{6}{m(m+1)} \quad (2.8)$$

is the central charge of the unitary minimal model  $\mathcal{M}_m$ . (More precisely, this holds in a double-scaling limit: pick  $\bar{r}$  and  $\bar{\theta}_0$  with  $-(m-2)\bar{\theta}_0/2 < \ln(\bar{r}) < -(m-3)\bar{\theta}_0/2$ , and set  $r = \bar{r}^\rho$  and  $\theta_0 = \rho\bar{\theta}_0$  with  $\rho > 0$ ; then  $\lim_{\rho \rightarrow \infty} c_{\text{eff}}(r, \theta_0) = c_m$ .) Furthermore, in the crossover region  $\ln(r) \approx -(m-3)\theta_0/2$  between the  $\mathcal{M}_m$  and  $\mathcal{M}_{m-1}$  plateaux, the staircase pseudoenergy  $\epsilon(\theta)$  tends uniformly on suitably-shifted intervals to the pseudoenergies  $\epsilon_i(\theta)$  which solve the system of TBA equations introduced in [16] to describe the  $\phi_{13}$ -induced flow from  $\mathcal{M}_m$  to  $\mathcal{M}_{m-1}$ , a

flow which had previously been found perturbatively in [17, 18]. (This interpolating theory was denoted by  $\mathcal{MA}_m^{(+)}$  in [16].) This is illustrated in figure 2 for  $m = 4$ .

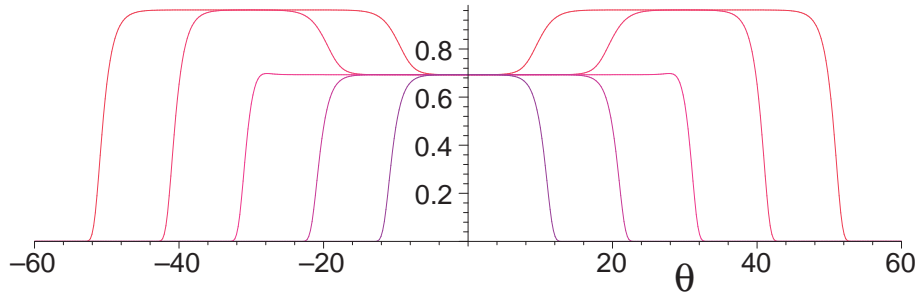


Figure 2: The function  $L(\theta)$  at various values of  $r$ , for  $\theta_0 = 60$ . From the upper to the lower curve,  $\ln(r)$  is equal to  $-50$ ,  $-40$ ,  $-30$ ,  $-20$  and  $-10$ . This range covers the crossover between tricritical and critical Ising models, and the form of  $L(\theta)$  around  $\theta = +30$  and  $-30$  approximates the functions  $\ln(1 + e^{-\epsilon_1(\theta-30)})$  and  $\ln(1 + e^{-\epsilon_2(\theta+30)})$  from the corresponding interpolating TBA of [16] (cf. figure 1 of [5]).

The natural interpretation of these results – also backed by perturbative studies, in the spirit of [17], at large  $m$  [19] – is that there is a one-parameter family of integrable quantum field theories with renormalisation group trajectories which, in the limit  $\theta_0 \rightarrow \infty$ , approach the union of the renormalisation group trajectories of the  $\mathcal{MA}_m^{(+)}$  theories. From now on we will assume this to be the case, and use it to deduce equations for the flow of the  $g$ -function in these same theories.

To treat the boundary staircase model using exact  $g$ -function techniques, we need a conjecture for its boundary reflection factor  $R(\theta)$ . It is natural to suppose that this can be obtained through the same analytic continuation of the sinh-Gordon boundary reflection factor as yielded the bulk S-matrix (2.1). The boundary sinh-Gordon model with no additional boundary degrees of freedom has a two-parameter family of integrable boundary conditions [20], and its reflection factor follows from that of the first sine-Gordon breather, found in [21] (see also, for example, [22]). Further continuing to the staircase values of the coupling, this leads to the following reflection factor:

$$R(\theta) = \frac{(\frac{1}{2})(\frac{3}{4} - \frac{i\theta_0}{2\pi})(\frac{3}{4} + \frac{i\theta_0}{2\pi})}{(\frac{1}{2} - \frac{E}{2})(\frac{1}{2} + \frac{E}{2})(\frac{1}{2} - \frac{F}{2})(\frac{1}{2} + \frac{F}{2})} \quad (2.9)$$

where  $E$  and  $F$  are two parameters whose relationship with the original two parameters of the boundary sinh-Gordon model will not be relevant below. In the sinh-Gordon model  $E$  and  $F$  are often real, but for the staircase model it will be more interesting to consider them at the complex values for which real-analyticity is preserved, as with the continuation of the bulk coupling. Hence we set

$$E = \frac{i\theta_{b1}}{\pi}, \quad F = \frac{i\theta_{b2}}{\pi} \quad (2.10)$$

with  $\theta_{b1}$  and  $\theta_{b2}$  real and, without loss of generality, non-negative. There is an obvious extension of this ansatz to incorporate  $n$  boundary parameters  $\theta_{b1} \dots \theta_{bn}$ :

$$R(\theta) = \frac{(\frac{1}{2})(\frac{3}{4} - \frac{i\theta_0}{2\pi})(\frac{3}{4} + \frac{i\theta_0}{2\pi})}{\prod_{k=1}^n (\frac{1}{2} - \frac{i\theta_{bk}}{2\pi})(\frac{1}{2} + \frac{i\theta_{bk}}{2\pi})}. \quad (2.11)$$

For  $n > 2$  this does not correspond to an integrable sinh-Gordon boundary condition of the simple form treated in [20], but it can be realised by the addition of a stack of  $n-2$  defects next to such a boundary [23, 24].

For all of its subtleties at intermediate scales, the boundary staircase model in the far infrared is simply a massive diagonal scattering theory, both in the bulk and at the boundary. Its exact

$g$ -function should therefore be given by the formula proposed in [1]. Explicitly, for a boundary at the end of a cylinder of circumference  $r = MR$ ,

$$\ln g(r) = \ln g_0(r) + \ln g_b(r) \quad (2.12)$$

where

$$\ln g_0(r) = \sum_{n=1}^{\infty} \frac{1}{2n} \int_{\mathbb{R}^n} \frac{d\theta_1}{1 + e^{\epsilon(\theta_1)}} \cdots \frac{d\theta_n}{1 + e^{\epsilon(\theta_n)}} \phi_S(\theta_1 + \theta_2) \phi_S(\theta_2 - \theta_3) \cdots \phi_S(\theta_n - \theta_1) \quad (2.13)$$

and

$$\ln g_b(r) = \frac{1}{2} \int_{\mathbb{R}} d\theta \left( \phi_b(\theta) - \phi_S(2\theta) - \frac{1}{2} \delta(\theta) \right) L(\theta) \quad (2.14)$$

where  $\epsilon(\theta)$  solves the TBA equation (2.2),  $L(\theta) = \ln(1 + e^{-\epsilon(\theta)})$ ,  $\phi_S(\theta) = -\frac{i}{2\pi} \frac{d}{d\theta} \ln S(\theta) = \phi(\theta - \theta_0) + \phi(\theta + \theta_0)$ , and, restricting attention to the  $n = 2$  case of (2.11) for simplicity,

$$\begin{aligned} \phi_b(\theta) &= -\frac{i}{2\pi} \frac{d}{d\theta} \ln R(\theta) \\ &= -\phi(\theta) + \phi_{(\frac{3}{4})}(\theta - \frac{1}{2}\theta_0) + \phi_{(\frac{3}{4})}(\theta + \frac{1}{2}\theta_0) \\ &\quad + \phi(\theta - \theta_{b1}) + \phi(\theta + \theta_{b1}) + \phi(\theta - \theta_{b2}) + \phi(\theta + \theta_{b2}). \end{aligned} \quad (2.15)$$

As in [5], this normalisation for  $\phi_b$  differs by a factor of two from that used in [1, 2]; we also used  $\phi(\theta) = -\phi_{(\frac{1}{2})}(\theta)$ . These equations are straightforward to implement numerically, and can also be treated analytically in various limits. In the next section we report some of the results of this analysis for the full staircase model, while in section 4 we show how the staircase  $g$ -function equations decompose in suitable limits into sets of equations which govern exact  $g$ -function flows in the interpolating theories  $\mathcal{MA}_m^{(+)}$ .

### 3 The boundary staircase flows

Following the split (2.12) of  $\ln g$  into the sum  $\ln g_0 + \ln g_b$ , the single-integral piece  $\ln g_b$  naturally splits into three further terms as  $\ln g_b = \ln g_{b1} + \ln g_{b2} + \ln g_{b3}$ , with

$$\ln g_{b1} = \frac{1}{2} \int_{\mathbb{R}} d\theta \left( -\phi(\theta) - \frac{1}{2} \delta(\theta) \right) L(\theta), \quad (3.1)$$

$$\ln g_{b2} = \frac{1}{2} \int_{\mathbb{R}} d\theta \left( \phi_{(\frac{3}{4})}(\theta - \frac{1}{2}\theta_0) + \phi_{(\frac{3}{4})}(\theta + \frac{1}{2}\theta_0) - \phi(2\theta - \theta_0) - \phi(2\theta + \theta_0) \right) L(\theta), \quad (3.2)$$

$$\ln g_{b3} = \frac{1}{2} \int_{\mathbb{R}} d\theta \left( \phi(\theta - \theta_{b1}) + \phi(\theta + \theta_{b1}) + \phi(\theta - \theta_{b2}) + \phi(\theta + \theta_{b2}) \right) L(\theta). \quad (3.3)$$

Notice that  $\ln g_{b1}$  and  $\ln g_{b2}$  are independent of the boundary parameters, and  $\ln g_{b1}$  only depends on the bulk parameter  $\theta_0$  implicitly, via the function  $L(\theta)$ .

In the large- $\theta_0$  limit, the full  $g$ -function passes through a series of plateaux as  $\ln r$  varies, its value on each plateau always matching a (conformal)  $g$ -function value, or a product of such values, for the conformal field theory seen by the bulk theory at that value of  $r$ . Some features of this behaviour can be seen in figure 3, where for simplicity the values of  $\theta_{b1}$  were chosen such that their associated boundary transitions always coincide with bulk transitions. These and other aspects will be analysed in more detail later.

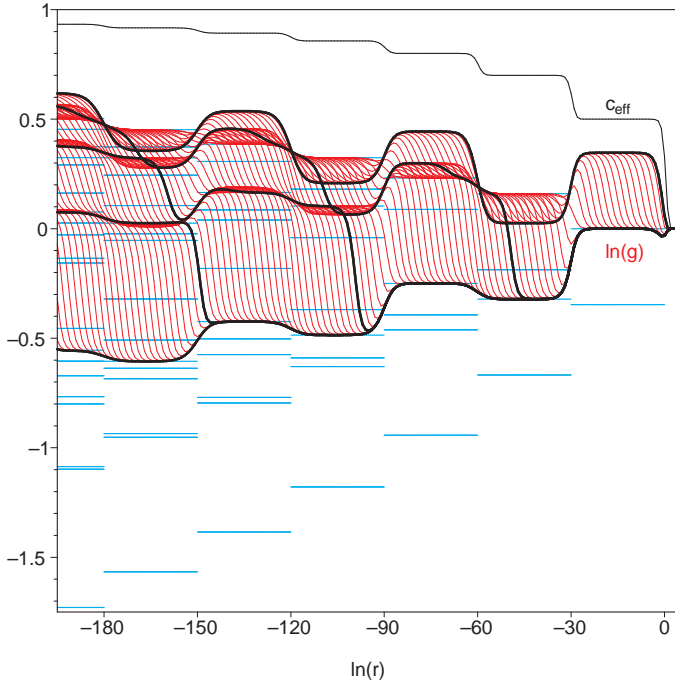


Figure 3a:  $\theta_{b1} = 0$ .

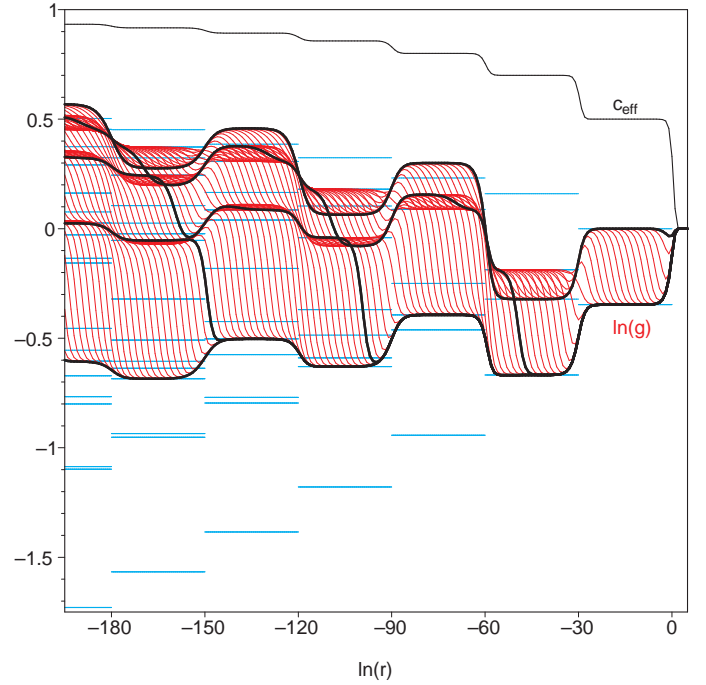


Figure 3b:  $\theta_{b1} = 60$ .

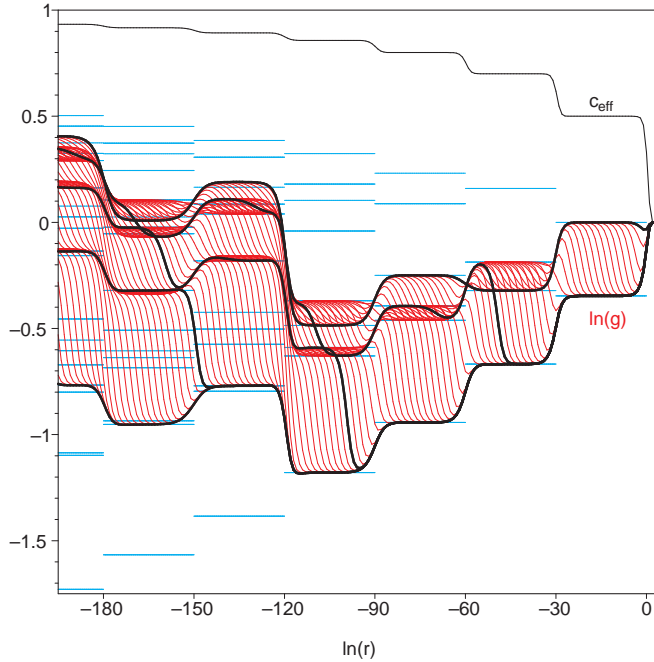


Figure 3c:  $\theta_{b1} = 120$ .

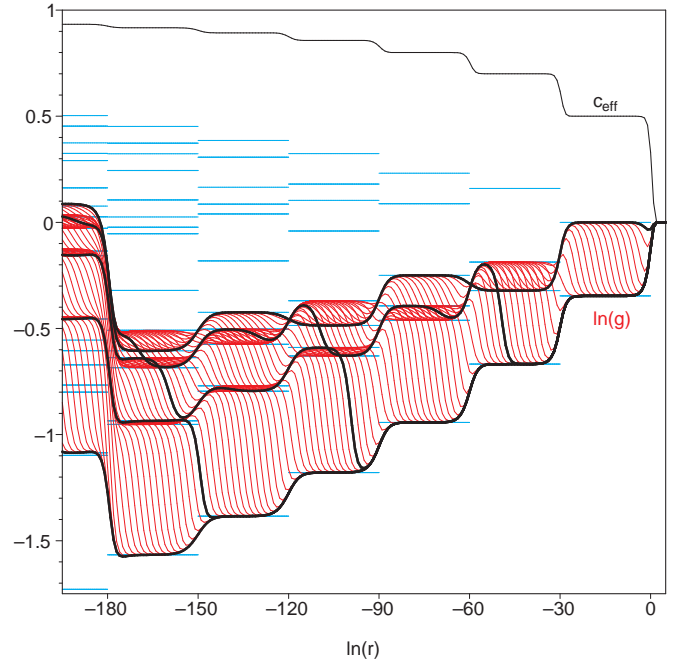


Figure 3d:  $\theta_{b1} = 180$ .

Figure 3: Staircase  $g$ -function flows for various values of  $\theta_{b1}$ . In each plot  $\theta_0 = 60$ , and the value of  $\theta_{b2}$  is scanned from 0 to 200 in steps of 2. To aid the eye five  $g$ -function flows have been highlighted. The lowest-lying of them has  $\theta_{b2} = 200$ ; reading from left to right, this is then joined by the flows for  $\theta_{b2} = 150, 100, 50$  and 0 respectively. The short horizontal lines (light blue online) show the logarithms of the conformal  $g$ -function values (3.5) for the ‘pure’ (Cardy) boundaries of each minimal model visited by the staircase flow. The other  $g$ -function plateaux correspond to superpositions of these boundaries, as discussed in the main text.

To give some precise formulae, we start by recalling some facts about the minimal model  $\mathcal{M}_m$  and its conformal boundary conditions. The model has central charge  $c_m = 1 - \frac{6}{m(m+1)}$ , and the permitted irreducible highest-weight representations of the Virasoro algebra are labelled by pairs of integers  $a$  and  $b$  with  $1 \leq a \leq m-1$  and  $1 \leq b \leq m$  subject to the identifications  $(a, b) \sim (m-a, m+1-b)$ . They have highest weight

$$h_{ab} = \frac{((m+1)a - mb)^2 - 1}{4m(m+1)}. \quad (3.4)$$

In particular the bulk field  $\phi_{13}$ , which induces the interpolating flow from  $\mathcal{M}_m$  to  $\mathcal{M}_{m-1}$ , has scaling dimension  $2h_{13} = 2(m-1)/(m+1)$ . The most general conformal boundary condition is a superposition of ‘pure’ (Cardy) boundary conditions [25]. There is one such boundary condition for each irreducible highest-weight representation (3.4), and its boundary entropy (or  $g$ -function) is [4]

$$g(m, a, b) = \left( \frac{8}{m(m+1)} \right)^{\frac{1}{4}} \frac{\sin(\frac{a\pi}{m}) \sin(\frac{b\pi}{m+1})}{\sqrt{\sin(\frac{\pi}{m}) \sin(\frac{\pi}{m+1})}}. \quad (3.5)$$

Notice that this formula respects the identification  $(a, b) \cong (m-a, m+1-b)$ , and has the additional symmetries  $g(m, a, b) = g(m, m-a, b)$  and  $g(m, a, b) = g(m, a, m+1-b)$ . This is the  $\mathbb{Z}_2$  ‘spin flip’ symmetry of minimal model boundary conditions which in the case of the Ising model maps between spin up and spin down Dirichlet boundaries. For superpositions of Cardy boundaries, the boundary entropies simply add.

We will also need some more detailed information about the form of the function  $L(\theta)$ , illustrated for some sample values of  $\ln(r)$  in figure 2. Suppose the bulk theory is near to the minimal model  $\mathcal{M}_m$ , so that  $\ln(r)$  satisfies

$$-(m-2)\theta_0/2 \ll \ln(r) \ll -(m-3)\theta_0/2. \quad (3.6)$$

Setting  $\alpha = 2\ln(1/r) - (m-3)\theta_0$ , we have  $0 \ll \alpha \ll \theta_0$  and, starting from  $\theta \approx \ln(1/r)$ ,  $L(\theta)$  exhibits an alternating series of plateaux of lengths  $\alpha$  and  $\theta_0 - \alpha$ , the  $i^{\text{th}}$  plateau being centred at  $\theta = z_i$ , where

$$z_i = (m-2-i)\theta_0/2, \quad i = 1, 2, \dots, 2m-5. \quad (3.7)$$

(For later comparison with the TBA systems for  $\mathcal{MA}_m^{(+)}$  it will be convenient to count these plateaux starting from the right.) The plateau values of  $L(\theta)$  can be found as explained in [13]. Adapting slightly the notation from [16, 26], define constants  $x_a$  and  $y_a$  by

$$1 + x_a = \frac{\sin^2\left(\frac{\pi a}{m+1}\right)}{\sin^2\left(\frac{\pi}{m+1}\right)}, \quad 1 + y_a = \frac{\sin^2\left(\frac{\pi a}{m}\right)}{\sin^2\left(\frac{\pi}{m}\right)}. \quad (3.8)$$

Starting from  $\theta = +\infty$ ,  $L(\theta)$  is close to 0 until  $\theta \approx \ln(1/r)$ , and then has height  $\ln(1+x_2)$  for  $\ln(1/r) - \alpha \ll \theta \ll \ln(1/r)$ , then  $\ln(1+y_2)$  for  $\ln(1/r) - \theta_0 \ll \theta \ll \ln(1/r) - \alpha$ , then  $\ln(1+x_3)$  for  $\ln(1/r) - \theta_0 - \alpha \ll \theta \ll \ln(1/r) - \theta_0$ , and so on, before returning to 0 for  $\theta \ll -\ln(1/r)$ . In full, the plateau values of  $L(\theta)$  are

$$\ln(1+x_a) : \quad z_{2a-3} - \alpha/2 \ll \theta \ll z_{2a-3} + \alpha/2, \quad a = 2 \dots m-1; \quad (3.9)$$

$$\ln(1+y_a) : \quad z_{2a-2} - (\theta_0 - \alpha)/2 \ll \theta \ll z_{2a-2} + (\theta_0 - \alpha)/2, \quad a = 2 \dots m-2, \quad (3.10)$$

and the complete sequence between  $\theta = -\ln(1/r)$  and  $\theta = +\ln(1/r)$  is

$$\{\ln(1+x_{m-1}), \ln(1+y_{m-2}), \ln(1+x_{m-2}), \ln(1+y_{m-3}) \dots \ln(1+y_2), \ln(1+x_2)\}. \quad (3.11)$$

As a shorthand we will refer to the intervals in the set (3.9) as  $x$ -type, and those in the set (3.10) as  $y$ -type. From (3.8),  $\ln(1+x_1) = \ln(1+y_1) = 0$ , and so we can formally add these two constants to the end of the sequence (3.11) while remaining consistent with the values taken by  $L(\theta)$  in the corresponding intervals, and likewise add  $\ln(1+y_{m-1})$  and then  $\ln(1+x_m)$  to the beginning. The symmetries  $x_a = x_{m+1-a}$ ,  $y_a = y_{m-a}$  reflect the more general symmetry  $L(\theta) = L(-\theta)$ .

With these preliminaries completed we return to the exact  $g$ -function  $g(r)$ . Three parts of  $\ln g(r)$  do not depend on the boundary parameters:  $\ln g_0$ ,  $\ln g_{b1}$  and  $\ln g_{b2}$ . These functions only undergo transitions at the values of  $\ln(r)$  where there is a bulk crossover, that is at  $\ln(r) = -(m-3)\theta_0/2$ ,  $m = 3, 4 \dots$ . The effective equations governing these transitions in the large- $\theta_0$  limit will be treated in the next section; here instead we will suppose that  $r$  satisfies (3.6) so that the bulk theory is close to the minimal model  $\mathcal{M}_m$ . Then  $g_0$ ,  $g_{b1}$  and  $g_{b2}$  are approximately constant, and given by the following formulae:

$$\ln g_0(r) = \begin{cases} \ln \left( \left( \frac{8}{m(m+1)} \right)^{\frac{1}{4}} \frac{\sin \frac{(m-1)\pi}{2m}}{\sqrt{\sin \frac{\pi}{m} \sin \frac{\pi}{m+1}}} \right) & \text{for } m \text{ odd} \\ \ln \left( \left( \frac{8}{m(m+1)} \right)^{\frac{1}{4}} \frac{\sin \frac{m\pi}{2(m+1)}}{\sqrt{\sin \frac{\pi}{m} \sin \frac{\pi}{m+1}}} \right) & \text{for } m \text{ even} \end{cases} \quad (3.12)$$

$$\ln g_{b1}(r) = -\frac{1}{2}L(0) = \begin{cases} -\frac{1}{2} \ln(1+x_{(m+1)/2}) = -\frac{1}{2} \ln \left( \frac{1}{\sin^2 \frac{\pi}{m+1}} \right) & \text{for } m \text{ odd} \\ -\frac{1}{2} \ln(1+y_{m/2}) = -\frac{1}{2} \ln \left( \frac{1}{\sin^2 \frac{\pi}{m}} \right) & \text{for } m \text{ even} \end{cases} \quad (3.14)$$

$$\ln g_{b2}(r) = -\frac{1}{2}L\left(\frac{1}{2}\theta_0\right) = \begin{cases} -\frac{1}{2} \ln(1+y_{(m-1)/2}) = -\frac{1}{2} \ln \left( \frac{\sin^2 \frac{(m-1)\pi}{2m}}{\sin^2 \frac{\pi}{m}} \right) & \text{for } m \text{ odd} \\ -\frac{1}{2} \ln(1+x_{m/2}) = -\frac{1}{2} \ln \left( \frac{\sin^2 \frac{m\pi}{2(m+1)}}{\sin^2 \frac{\pi}{m+1}} \right) & \text{for } m \text{ even.} \end{cases} \quad (3.16)$$

These results are exact in the limit  $\{\theta_0 \rightarrow \infty, -(m-2)\theta_0/2 \ll \ln(r) \ll -(m-3)\theta_0/2\}$ . The formula for  $\ln g_0$  will be derived in section 4 below. Those for  $\ln g_{b1}$  and  $\ln g_{b2}$  follow from the fact that  $\phi(\theta)$  and  $\phi_{(x)}(\theta)$  are only significantly non-zero near to  $\theta = 0$ . This means that the integrals (3.1) and (3.2) only receive contributions from the regions  $\theta \approx 0$  and  $\theta \approx \theta_0/2$ , where  $L(\theta)$  is, by (3.9) and (3.10), approximately constant. Pulling  $L(\theta)$  out of each integral and using

$$\int_{\mathbb{R}} d\theta \phi(\theta) = - \int_{\mathbb{R}} d\theta \phi_{(\frac{1}{2})}(\theta) = \frac{1}{2}, \quad \int_{\mathbb{R}} d\theta \phi_{(\frac{3}{4})}(\theta) = -\frac{1}{4} \quad (3.18)$$

together with the plateau values given by (3.9) and (3.10) leads to (3.14) – (3.17).

When  $\ln g_0$ ,  $\ln g_{b1}$  and  $\ln g_{b2}$  are summed, the pieces which depend on whether  $m$  is odd or even cancel, leaving the following simple result, valid for all values of  $m$ :

$$\ln g_0 + \ln g_{b1} + \ln g_{b2} = \ln \left( \left( \frac{8}{m(m+1)} \right)^{\frac{1}{4}} \sqrt{\sin \frac{\pi}{m} \sin \frac{\pi}{m+1}} \right). \quad (3.19)$$

This is the logarithm of  $g(m, 1, 1)$  or  $g(m, m-1, 1)$ , the boundary entropy of the conformal boundary condition associated with the bulk vacuum field or its  $\mathbb{Z}_2$  spin flip conjugate. In fact



it is not surprising that this partial sum should be equal to the logarithm of the full boundary entropy for some boundary condition, as will become clear as we examine the behaviour of the remaining part of  $\ln g$ , namely  $\ln g_{b_3}$ .

Since  $\ln g_{b_3}$  depends on the boundary parameters, we would expect it to undergo transitions not just where the bulk crossovers occur, but also, possibly, at energy scales related to pure-boundary transitions, and this turns out to be the case. The integral (3.3) receives contributions from  $\theta \approx \pm\theta_{b_1}$  and  $\theta \approx \pm\theta_{b_2}$ ; if these regions lie within the  $x$ - and  $y$ -type intervals (3.9) and (3.10) then, pulling  $L(\theta)$  outside the integrals and recalling that  $L(\theta) = L(-\theta)$ ,

$$\ln g_{b_3}(r) = \frac{1}{2} (L(\theta_{b_1}) + L(\theta_{b_2})) \quad (3.20)$$

and the value of  $\ln g_{b_3}(r)$  will not change for small changes in  $r$ . Conversely,  $\ln g_{b_3}(r)$  will undergo a crossover whenever  $r$  is such that either  $\theta_{b_1}$  or  $\theta_{b_2}$  lies on a boundary between the intervals (3.9) and (3.10). This means that there will be boundary transitions associated with the parameter  $\theta_{b_1}$  at

$$\ln(r) = -k\theta_0 - \theta_{b_1}, \quad k = 0, 1, \dots \quad (3.21)$$

and

$$\ln(r) = -k\theta_0 + \theta_{b_1}, \quad k = A, A+1, \dots \quad (3.22)$$

where  $A = \lceil 2\theta_{b_1}/\theta_0 \rceil$ , the smallest integer greater than or equal to  $2\theta_{b_1}/\theta_0$ . An analogous formula holds for  $\theta_{b_2}$ .

If  $\ln(1/r)$  is smaller than  $\theta_{b_1}$ ,  $L(\theta)$  is effectively zero near to  $\theta = \pm\theta_{b_1}$  and the term  $\frac{1}{2}L(\theta_{b_1})$  ceases to contribute to  $\ln g_{b_3}(r)$ . This explains why the plots in figure 3 stabilise with increasing  $\theta_{b_1}$ , with the parts of the plots with  $\ln(r) > -\theta_{b_1}$  being independent of  $\theta_{b_1}$ . If  $\ln(1/r)$  is smaller than  $\theta_{b_1}$  and  $\theta_{b_2}$ , then  $\ln g_{b_3}(r)$  is zero and the logarithm of the full  $g$ -function is given by the sum  $\ln g_0(r) + \ln g_{b_1}(r) + \ln g_{b_2}(r)$ , which we already observed was equal to  $\ln g(m, 1, 1)$  when the bulk theory is on the plateau corresponding to  $\mathcal{M}_m$ . If the limit  $\theta_{b_1} \rightarrow \infty, \theta_{b_2} \rightarrow \infty$  is taken *before*  $r$  is varied, we see that there is one flow which simply moves through the (1, 1) boundary conditions in the successive minimal models, its  $g$ -function being given by  $\ln g(r) = \ln g_0(r) + \ln g_{b_1}(r) + \ln g_{b_2}(r)$  for *all* values of  $r$ . (This is why the partial sum (3.19) is itself the logarithm of a boundary entropy.) For  $\ln(r) > -180$ , this flow is matched by the lowest-lying curve of figure 3d. Notice that since  $\ln g_{b_3}(r)$  is manifestly positive, all other  $g$ -function flows must lie above this limiting curve, an off-critical generalisation of the fact that at a fixed point the lowest-possible boundary entropy is always found for the (1, 1) boundary condition.

For smaller values of  $\theta_{b_1}$  and  $\theta_{b_2}$  the picture becomes more complicated, as can already be seen from figure 3. Nevertheless it is still possible to formulate general rules for the boundary conditions which are visited. The plateau behaviour of  $L(\theta)$  means that the sequence of boundary conditions seen for any given  $\theta_{b_1}$  and  $\theta_{b_2}$  depends on the intervals (3.9) and (3.10) that they (and their negatives) find themselves in as  $\ln(r)$  varies. From (3.11) and the immediately-following remarks, the possible values of  $L(\theta)$  on these intervals are the elements of the set

$$\{\ln(1 + x_a), \ln(1 + y_b)\} \quad (3.23)$$

where the indices  $a$  and  $b$  lie in the ranges

$$a \in \{1, \dots, m\}, \quad b \in \{1, \dots, m-1\} \quad (3.24)$$

and the value of 0, found for  $|\theta| \gg \ln(1/r)$ , arises when  $a$  is equal to 1 or  $m$ , or  $b$  is equal to 1 or  $m-1$ . The symmetries  $x_{m+1-a} = x_a, y_{m-b} = y_b$  could have been used to restrict the indices  $a$  and  $b$  to

$$\begin{aligned} & a \in \{1, \dots, \frac{m+1}{2}\}, \quad b \in \{1, \dots, \frac{m-1}{2}\} && \text{for } m \text{ odd} \\ \text{and} & && \\ & a, b \in \{1, \dots, \frac{m}{2}\} && \text{for } m \text{ even} \end{aligned} \quad (3.25)$$

but for reasons to be explained below it will be convenient to keep with the larger ranges. A given pair of boundary parameters corresponds to two (possibly equal) values of  $L(\theta)$  from the set (3.23), and, via the exponential of (3.20) and (3.19), to a value for the  $g$ -function. We found that this value can always be expressed as a sum of Cardy  $g$ -function values (3.5), according to the following rules, where we introduce the convenient notation  $[x_a, y_b]$  and so on to denote the particular combinations of boundary conditions which arise:

$$\begin{array}{lll}
L(\theta_{b1}) & L(\theta_{b2}) & \text{Boundary condition} \\
\ln(1+x_a) & \ln(1+y_b) & [x_a, y_b] \equiv (b, a) \\
\ln(1+x_p) & \ln(1+x_q) & [x_p, x_q] \equiv (1, |p-q|+1)\&(1, |p-q|+3)\&\cdots\&(1, m-|p+q-m-1|) \\
\ln(1+y_r) & \ln(1+y_s) & [y_r, y_s] \equiv (|r-s|+1, 1)\&( |r-s|+3, 1)\&\cdots\&(m-1-|r+s-m|, 1)
\end{array} \tag{3.26}$$

with the same result for  $\theta_{b1} \leftrightarrow \theta_{b2}$ . Notice that if all indices are restricted to the reduced ranges (3.25), the rules simplify to

$$\begin{array}{lll}
L(\theta_{b1}) & L(\theta_{b2}) & \text{Boundary condition} \\
\ln(1+x_a) & \ln(1+y_b) & (b, a) \\
\ln(1+x_p) & \ln(1+x_q) & (1, |p-q|+1)\&(1, |p-q|+3)\&\cdots\&(1, p+q-1) \\
\ln(1+y_r) & \ln(1+y_s) & (|r-s|+1, 1)\&( |r-s|+3, 1)\&\cdots\&(r+s-1, 1).
\end{array} \tag{3.27}$$

The identifications of  $g$ -function values with specific boundary conditions implied by (3.26) should be treated with care for a couple of reasons. First, ambiguity arises from the equalities  $g(m, a, b) = g(m, m-a, b)$ ,  $g(m, a, b) = g(m, a, m+1-b)$ . These are related to the symmetries  $L(\theta) = L(-\theta)$ ,  $x_a = x_{m+1-a}$ ,  $y_a = y_{m-a}$  of  $L(\theta)$  and its plateau values, and, more precisely, to the following symmetries of the boundary condition combinations given in (3.26):

$$\begin{array}{ll}
[x_a, y_b] = [x_{m+1-a}, y_{m-b}] & \overline{[x_a, y_b]} = [x_{m+1-a}, y_b] = [x_a, y_{m-b}] \\
[x_p, x_q] = [x_{m+1-p}, x_{m+1-q}] & \overline{[x_p, x_q]} = [x_{m+1-p}, x_q] = [x_p, x_{m+1-q}] \\
[y_r, y_s] = [y_{m-r}, y_{m-s}] & \overline{[y_r, y_s]} = [y_{m-r}, y_s] = [y_r, y_{m-s}]
\end{array} \tag{3.28}$$

where the overbar denotes the  $\mathbb{Z}_2$  ‘spin flip’ symmetry mentioned just after (3.5), acting on individual Cardy boundaries as  $\overline{(a, b)} = (m-a, b) \equiv (a, m+1-b)$ . As remarked in [5], it should be possible to resolve such ambiguities in a systematic fashion by studying the renormalisation group flows of the inner products of finite-volume excited states [27,28] with the boundary states, but we shall leave this for future work. Second, there are sometimes further, more accidental, degeneracies in the set of non-negative-integer sums of Cardy  $g$ -function values – for example,  $g(5, 1, 3) = 2g(5, 1, 1)$ , so that in  $\mathcal{M}_5$  the (1, 3) and (1, 1)&(1, 1) boundary conditions cannot be distinguished by their  $g$ -function values alone. Nevertheless, and modulo the spin flip ambiguity just described, (3.26) is the only set of decompositions we have found which works in a uniform fashion for all  $m$ . From now on we shall assume that it is correct, and mostly leave the spin flip ambiguity implicit.

Continuing to suppose that the bulk theory is in the vicinity of the bulk fixed point  $\mathcal{M}_m$ , we now let  $\ln(r)$  vary from the lower to the upper end of the range (3.6), that is from  $-(m-2)\theta_0/2$  to  $-(m-3)\theta_0/2$ . The centres of the intervals (3.9) and (3.10) remain fixed, at  $\theta = z_i$ ,  $i = 1 \dots 2m-5$ , but the widths of the  $x$ -type intervals,  $\alpha \equiv 2\ln(1/r) - (m-3)\theta_0$ , decrease from  $\theta_0$  to zero, while those of the  $y$ -type intervals,  $\theta_0 - \alpha$ , increase from zero to  $\theta_0$ . Thus so long as  $|\theta_{b1}| < (m-2)\theta_0/2$  and  $\theta_{b1}$  is not an integer multiple of  $\theta_0/2$ , the regions  $\theta \approx \pm\theta_{b1}$  move from  $x$ -type intervals to  $y$ -type intervals during this process, and the value of  $L(\pm\theta_{b1})$ , and hence that of the  $g$ -function, undergoes a change. For brevity we will phrase the rest of the discussion in terms of the intervals seen by  $L(\theta_{b1})$ , but we could equally look at  $L(-\theta_{b1})$ . By the  $\mathbb{Z}_2$  ambiguity just discussed this might lead to different boundary conditions being assigned but since the  $g$ -functions are blind to

their difference, we will ignore this issue for now. In fact, it will be convenient to allow  $\theta_{b_1}$  (and  $\theta_{b_2}$ ) to take positive and negative values, so all options are in any case covered.

Suppose, then, that at the start of the process  $\theta_{b_1}$  is in the  $x$ -type interval centred at  $\theta = z_{2r-3}$ , and  $\theta_{b_2}$  is in the  $x$ -type interval centred at  $\theta = z_{2s-3}$ , corresponding to plateau values for  $L(\theta_{b_1})$  and  $L(\theta_{b_2})$  equal to  $\ln(1+x_r)$  and  $\ln(1+x_s)$  respectively. The  $y$ -type interval that  $\theta_{b_1}$  moves to depends on its position relative to  $z_{2r-3}$ . If  $\theta_{b_1} > z_{2r-3}$  then  $L(\theta_{b_1})$  moves to the plateau  $\ln(1+y_{r-1})$ , while if  $\theta_{b_1} < z_{2r-3}$  it moves to the plateau  $\ln(1+y_r)$ . An identical set of possibilities occurs for  $L(\theta_{b_2})$ , with a transition which may occur before or after that in  $L(\theta_{b_1})$  depending on the relative distances of  $\theta_{b_1}$  and  $\theta_{b_2}$  from the centres of their original ( $x$ -type) intervals. Putting these ingredients together gives the following ‘skeleton’ of transitions from an initial situation where  $L(\theta_{b_1}) = \ln(1+x_r)$  and  $L(\theta_{b_2}) = \ln(1+x_s)$ :

$$\begin{array}{ccccc}
 [y_r, y_s] & \longleftarrow & [x_r, y_s] & \longrightarrow & [y_{r-1}, y_s] \\
 \uparrow & & \uparrow & & \uparrow \\
 [y_r, x_s] & \longleftarrow & [x_r, x_s] & \longrightarrow & [y_{r-1}, x_s] \\
 \downarrow & & \downarrow & & \downarrow \\
 [y_r, y_{s-1}] & \longleftarrow & [x_r, y_{s-1}] & \longrightarrow & [y_{r-1}, y_{s-1}]
 \end{array}$$

This diagram encapsulates the boundary flows seen while the bulk is in the vicinity of  $\mathcal{M}_m$ , if  $\theta_{b_1}$  and  $\theta_{b_2}$  are in the intervals  $[z_{2r-3} - \theta_0/2, z_{2r-3} + \theta_0/2]$ ,  $[z_{2s-3} - \theta_0/2, z_{2s-3} + \theta_0/2]$ . The complete set of flows seen near to  $\mathcal{M}_m$  is the union of a number of such diagrams, so as to cover the full ranges  $|\theta_{b_1}| \leq (m-2)\theta_0/2$ ,  $|\theta_{b_2}| \leq (m-2)\theta_0/2$ . To give one example, at  $m = 5$  this results in a  $7 \times 7$  grid, the lower ( $\theta_{b_2} \geq 0$ ) half of which is:

$$\begin{array}{cccccccc}
 \vdots & & \vdots & & \vdots & & \vdots & & \vdots \\
 [y_4, x_3] & \longleftarrow & [x_4, x_3] & \longrightarrow & [y_3, x_3] & \longleftarrow & [x_3, x_3] & \longrightarrow & [y_2, x_3] & \longleftarrow & [x_2, x_3] & \longrightarrow & [y_1, x_3] \\
 \downarrow & & \downarrow & & \downarrow & & \downarrow & & \downarrow & & \downarrow & & \downarrow \\
 [y_4, y_2] & \longleftarrow & [x_4, y_2] & \longrightarrow & [y_3, y_2] & \longleftarrow & [x_3, y_2] & \longrightarrow & [y_2, y_2] & \longleftarrow & [x_2, y_2] & \longrightarrow & [y_1, y_2] \\
 \uparrow & & \uparrow & & \uparrow & & \uparrow & & \uparrow & & \uparrow & & \uparrow \\
 [y_4, x_2] & \longleftarrow & [x_4, x_2] & \longrightarrow & [y_3, x_2] & \longleftarrow & [x_3, x_2] & \longrightarrow & [y_2, x_2] & \longleftarrow & [x_2, x_2] & \longrightarrow & [y_1, x_2] \\
 \downarrow & & \downarrow & & \downarrow & & \downarrow & & \downarrow & & \downarrow & & \downarrow \\
 [y_4, y_1] & \longleftarrow & [x_4, y_1] & \longrightarrow & [y_3, y_1] & \longleftarrow & [x_3, y_1] & \longrightarrow & [y_2, y_1] & \longleftarrow & [x_2, y_1] & \longrightarrow & [y_1, y_1]
 \end{array}$$

The entries in square brackets can be converted into specific boundary conditions by using the dictionary (3.26), to give the picture shown in figure 4 below. We note once more that these predictions are made modulo the  $\mathbb{Z}_2$  ambiguity in the relationship between  $g$ -function values and boundary conditions. The options chosen here, which follow from the rule formulated earlier, are consistent with predictions made in, for example, [9, 29], but we have not attempted to confirm them using exact  $g$ -function techniques. As already mentioned, this would require the computation of inner products of states other than the ground state with the boundary state.

Notice that the figure is symmetrical about the diagonals  $\theta_{b_1} = \theta_{b_2}$  and  $\theta_{b_1} = -\theta_{b_2}$ , while negating either  $\theta_{b_1}$  or  $\theta_{b_2}$  individually has the same effect as the  $\mathbb{Z}_2$  spin flip. This second feature means that the boundary conditions in the middle column on the figure,  $\theta_{b_1} = 0$  (or equivalently,

the top row shown,  $\theta_{b2} = 0$ ) are mapped into themselves under the spin flip. As follows from (3.28), the corresponding properties hold for all other values of  $m$ , if it is assumed that the rules (3.26) are correct in general.

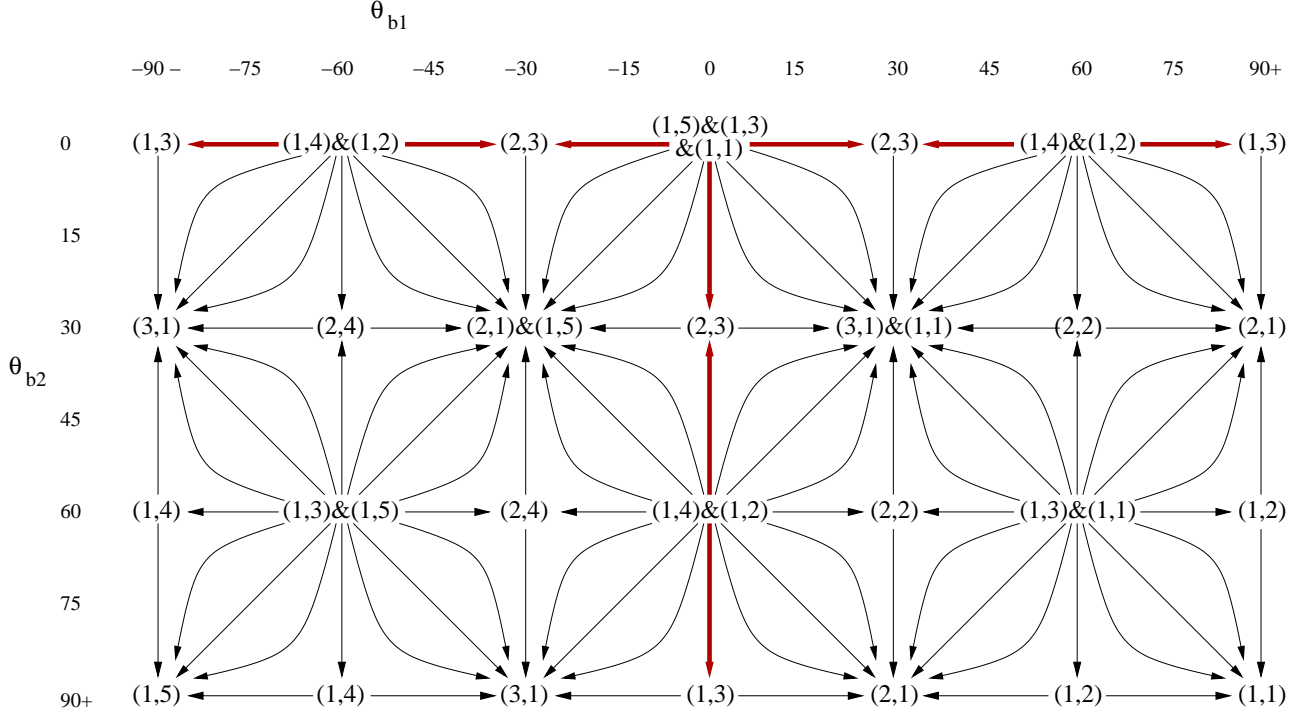


Figure 4: A diagram of the pure boundary flows appearing near to the bulk fixed point  $\mathcal{M}_5$ , for  $\theta_0 = 60$  and various values of  $\theta_{b1}$  and  $\theta_{b2}$ . The slightly-thicker vertical and horizontal arrows (red online) indicate the flows and boundary conditions which are mapped to themselves under the  $\mathbb{Z}_2$  spin flip.

To complete the picture we must examine what happens when the bulk theory moves between two neighbouring fixed points, say  $\mathcal{M}_m$  and  $\mathcal{M}_{m-1}$ . The bulk flow occurs when  $\ln(r)$  varies through a region centred on  $\ln(r) = -(m-3)\theta_0/2$  which is of size of order one as  $\theta_0 \rightarrow \infty$ . As this happens the form of  $L(\theta)$  changes: the  $x$ -type plateaux for  $\mathcal{M}_m$  shrink to zero size, while the  $y$ -type plateau of height  $\ln(1+y_a)|_{\mathcal{M}_m}$ ,  $a = 1 \dots m-1$ , for  $\mathcal{M}_m$  becomes the  $x$ -type plateau  $\ln(1+x_a)|_{\mathcal{M}_{m-1}}$  for  $\mathcal{M}_{m-1}$ , with  $y$ -type plateaux for  $\mathcal{M}_{m-1}$  opening up between these as  $\ln(r)$  increases further. (By (3.8),  $\ln(1+y_a)|_{\mathcal{M}_m} = \ln(1+x_a)|_{\mathcal{M}_{m-1}}$ , so there is no sudden change in heights implied by the redesignation of  $y$ -type to  $x$ -type plateaux over the transition.)

Now consider the behaviour of the logarithm of the full  $g$ -function,  $\ln g = \ln g_0 + \ln g_{b1} + \ln g_{b2} + \ln g_{b3}$ , as  $\mathcal{M}_m$  flows to  $\mathcal{M}_{m-1}$ . From (3.19), the sum of the first three terms,  $\ln g_0 + \ln g_{b1} + \ln g_{b2}$ , changes from  $\ln g(m, 1, 1)$  to  $\ln g(m-1, 1, 1)$ . The behaviour of the remaining piece,  $\ln g_{b3}$ , depends on the values of  $\theta_{b1}$  and  $\theta_{b2}$ . Suppose first that both  $|\theta_{b1}| \leq (m-3)\theta_0/2$  and  $|\theta_{b2}| \leq (m-3)\theta_0/2$ , so that neither boundary parameter has become decoupled at the point of the bulk transition under discussion. There are then three cases:

(i) If neither  $\theta_{b1}$  nor  $\theta_{b2}$  are at the centre of what had been an  $x$ -type plateau for  $\mathcal{M}_m$ , that is if

$$\theta_{b1}, \theta_{b2} \neq (m-3)\theta_0/2 - k\theta_0, \quad k = 0, 1, \dots, m-3 \quad (3.29)$$

then both  $\theta_{b1}$  and  $\theta_{b2}$  will have undergone a ‘pure-boundary’ transition of the sort described earlier, from an  $x$ -type onto a  $y$ -type plateau, *before* the  $\mathcal{M}_m \rightarrow \mathcal{M}_{m-1}$  transition is reached. Thus the conformal boundary condition seen just before the bulk transition occurs will correspond to some pair  $[y_r, y_s]|_{\mathcal{M}_m}$  where  $2 \leq r, s \leq m-2$ , corresponding to  $\theta_{b1}$  and  $\theta_{b2}$  lying in the intervals  $((m-3)\theta_0/2 - (r-1)\theta_0, (m-3)\theta_0/2 - (r-2)\theta_0)$  and  $((m-3)\theta_0/2 - (s-1)\theta_0, (m-3)\theta_0/2 - (s-2)\theta_0)$ .

After the transition the plateau values will not have changed but their interpretations will have, to the pair  $[x_r, x_s]_{\mathcal{M}_{m-1}}$ . Translated into specific conformal boundary conditions using (3.26) at  $m$  and  $m-1$  the flow is therefore

$$\begin{aligned} (f, 1) \& (f+2, 1) \& \cdots \& (g, 1) & \mathcal{M}_m \\ \downarrow & & & & \\ (1, f) \& (1, f+2) \& \cdots \& (1, g) & \mathcal{M}_{m-1} \end{aligned} \quad (3.30)$$

where

$$f = |r-s|+1, \quad g = m-1-|r+s-m| \quad \text{and} \quad 2 \leq r, s \leq m-2. \quad (3.31)$$

Via (3.28) and the symmetry under  $\theta_{b1} \leftrightarrow \theta_{b2}$  the full set of options is explored by restricting  $r$  and  $s$  to the fundamental domain  $2 \leq r \leq s \leq m-2$ ,  $r+s \leq m$ . In fact, (3.31) is equivalent to  $f$  and  $g$  in (3.30) being restricted by

$$1 \leq f < g \leq m-1, \quad f-g \in 2\mathbb{Z}. \quad (3.32)$$

Notice that these, the generic flows, always start at ‘sinks’ on networks of pure-boundary flows such as figure 4, and end on ‘sources’ on the corresponding network one minimal model down.

(ii) If one of  $\theta_{b1}$  or  $\theta_{b2}$  lies at the centre of an  $x$ -type plateau for  $\mathcal{M}_m$ , then it remains on that plateau right up to the moment of the bulk transition, after which it will instead lie in the centre of a  $y$ -type plateau for  $\mathcal{M}_{m-1}$ . If this centre is located at  $\theta = (m-3)\theta_0/2 - (s-2)\theta_0$ ,  $2 \leq s \leq m-1$ , then the corresponding value of  $L(\theta)$  moves from  $\ln(1+x_s)|_{\mathcal{M}_m}$  to  $\ln(1+y_{s-1})|_{\mathcal{M}_{m-1}}$ . The other plateau value simply changes its designation from  $\ln(1+y_r)|_{\mathcal{M}_m}$  to  $\ln(1+x_r)|_{\mathcal{M}_{m-1}}$ , as in case (i). Thus the boundary condition flow is  $[x_s, y_r]_{\mathcal{M}_m} \rightarrow [y_{s-1}, x_r]_{\mathcal{M}_{m-1}}$ , or

$$\begin{aligned} (r, s) & \mathcal{M}_m \\ \downarrow & \\ (s-1, r) & \mathcal{M}_{m-1} \end{aligned} \quad (3.33)$$

where

$$2 \leq r \leq m-2, \quad 2 \leq s \leq m-1. \quad (3.34)$$

(iii) Lastly, if both  $\theta_{b1}$  and  $\theta_{b2}$  are at the centres of  $x$ -type plateaux for  $\mathcal{M}_m$ , say at  $(m-3)\theta_0/2 - (r-2)\theta_0$  and  $(m-3)\theta_0/2 - (s-2)\theta_0$  with  $2 \leq r, s \leq m-1$ , then reasoning as above the boundary condition flow is  $[x_r, x_s]_{\mathcal{M}_m} \rightarrow [y_{r-1}, y_{s-1}]_{\mathcal{M}_{m-1}}$ , or

$$\begin{aligned} (1, f) \& (1, f+2) \& \cdots \& (1, g) & \mathcal{M}_m \\ \downarrow & & & & \\ (f, 1) \& (f+2, 1) \& \cdots \& (g-2, 1) & \mathcal{M}_{m-1} \end{aligned} \quad (3.35)$$

where this time

$$f = |r-s|+1, \quad g = m-|r+s-m-1| \quad \text{and} \quad 2 \leq r, s \leq m-1, \quad (3.36)$$

or equivalently

$$1 \leq f < g \leq m, \quad f-g \in 2\mathbb{Z}. \quad (3.37)$$

For these (least-generic) cases the flows are always from sources to sinks on neighbouring pairs of pure-boundary networks such as figure 4, and decrease by one the number of superposed Cardy states.

Finally we must treat the cases where either one or both of  $|\theta_{b1}|$  and  $|\theta_{b2}|$  is larger than  $(m-3)\theta_0/2$ . Then the corresponding plateau values of  $L(\theta)$  simply flow from zero to zero. If

in addition neither  $\theta_{b_1}$  nor  $\theta_{b_2}$  lie at the centre of an  $x$ -type plateau, then it is easily seen that the situation is covered by case (i) above, if the indices  $r$  and  $s$  are allowed to take the additional values of 1 and  $m-1$  (recall that  $\ln(1+y_1)|_{\mathcal{M}_m} = \ln(1+y_{m-1})|_{\mathcal{M}_m} = \ln(1+x_1)|_{\mathcal{M}_{m-1}} = \ln(1+x_{m-1})|_{\mathcal{M}_{m-1}} = 0$ ). Thus the combined story is that there are flows of the form (3.30) for every pair  $(f, g)$  satisfying

$$1 \leq f \leq g \leq m-1, \quad f-g \in 2\mathbb{Z}. \quad (3.38)$$

(Taking  $f = g = 1$  or  $f = g = m-1$  gives the flows  $(1, 1)|_{\mathcal{M}_m} \rightarrow (1, 1)|_{\mathcal{M}_{m-1}}$  and  $(m-1, 1)|_{\mathcal{M}_m} \rightarrow (1, m-1)|_{\mathcal{M}_{m-1}}$  which occur when both  $|\theta_{b_1}|$  and  $|\theta_{b_2}|$  are larger than  $(m-3)\theta_0/2$ , so that  $\ln g_{b_3}$  remains zero throughout the flow.) Last of all, if, say,  $|\theta_{b_2}| > (m-3)\theta_0/2$  while  $\theta_{b_1}$  is at the centre of an  $x$ -type plateau, then the flow is  $[y_1, x_s]|_{\mathcal{M}_m} \rightarrow [x_1, y_{s-1}]|_{\mathcal{M}_{m-1}}$  or  $[y_{m-1}, x_s]|_{\mathcal{M}_m} \rightarrow [x_{m-1}, y_{s-1}]|_{\mathcal{M}_{m-1}}$  with  $2 \leq s \leq m-1$ , which simply means that the indices in (3.33) can be given the enlarged range

$$1 \leq r \leq m-1, \quad 2 \leq s \leq m-1. \quad (3.39)$$

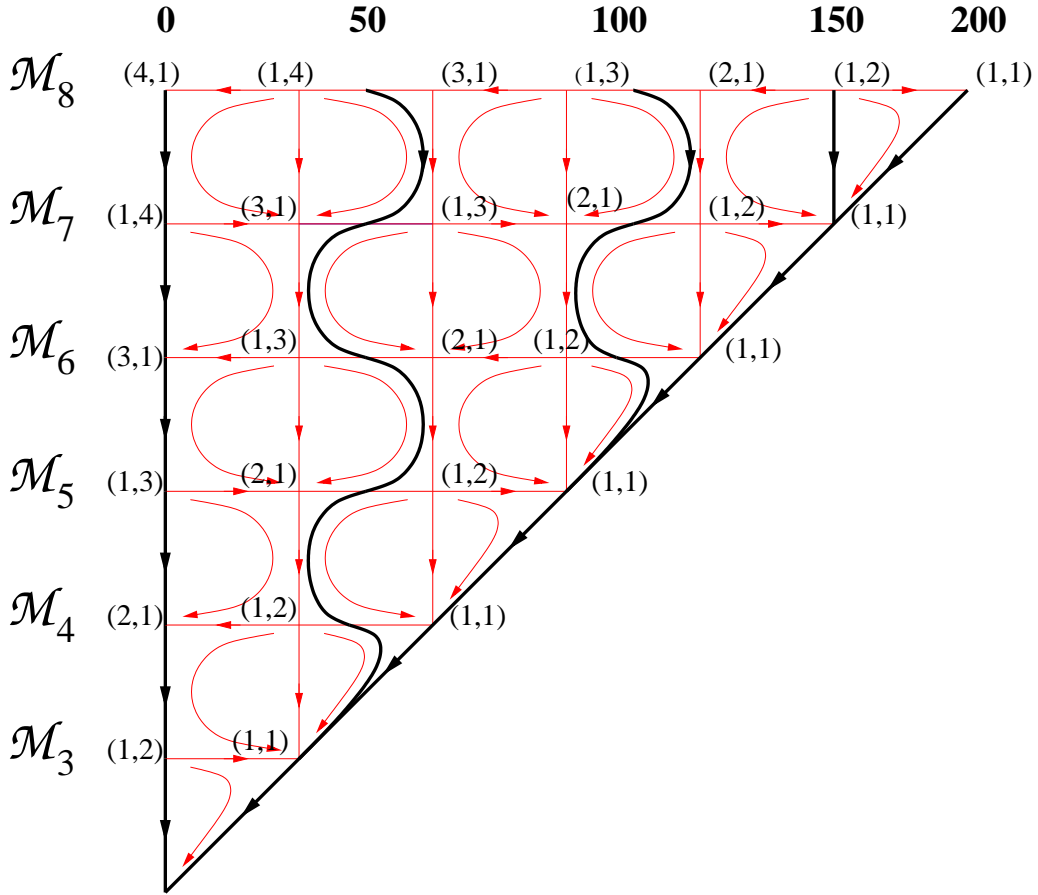


Figure 5: A depiction of the flows corresponding to figure 3d, for which  $\theta_{b_1} = 180$  and  $\theta_{b_2} = 0 \dots 200$ . The rows are labelled by the corresponding bulk minimal model; nodes are then labelled by the boundary condition within that model. The highlighted flows, labelled in bold along the top of the figure, correspond to the values of  $\theta_{b_2}$  that were also highlighted in figure 3d. Although some flow lines appear to cross, this is an artifact of the projection onto the page, and does not occur in the full multidimensional space of flows.

These rules can be combined to understand the sequences of  $g$ -function flows seen in figure 3 and further illustrated in figures 5 and 6. Consider  $\theta_{b_1} = 180$ ,  $\theta_{b_2} = 50$ , one of the highlighted flows in figures 3d and 5. Focussing on the part of the flow beginning at  $\mathcal{M}_8$ , the initial  $g$ -function

value is close to that of the boundary condition (1, 4). Since  $\theta_{b_1} > \ln(1/r)$  everywhere in this part of the flow, only  $\theta_{b_2}$  has an effect on the subsequent trajectory. The centre of the  $L(\theta)$  plateau associated with the boundary condition (1, 4) at  $\mathcal{M}_8$  is at  $\theta = 30$ , and since  $\theta_{b_2} > 30$  the flow within  $\mathcal{M}_8$  is to (3, 1). Then as the bulk theory flows from  $\mathcal{M}_8$  to  $\mathcal{M}_7$ , the boundary condition flows to (1, 3). The centre of the associated  $L(\theta)$  plateau is then at  $\theta = 60$ , and since  $\theta_{b_2} < 60$ , the flow within  $\mathcal{M}_7$  is then towards (3, 1), and so on. Repeating this exercise for other values of  $\theta_{b_2}$  leads to the set of flows illustrated in figure 5, the second highlighted flow of which corresponds to  $\theta_{b_2} = 50$ . Note that the pure-boundary flows within  $\mathcal{M}_5$  on figure 5 match the flows on the bottom row of figure 4.

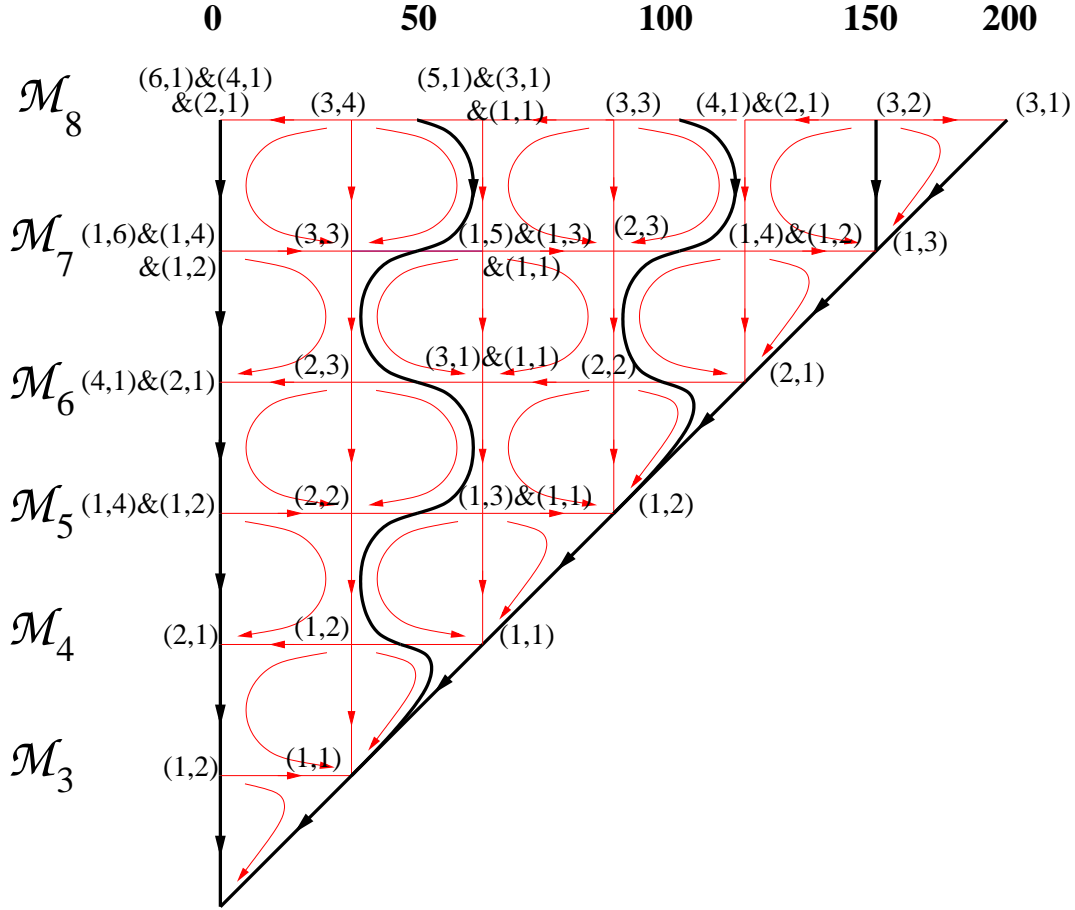


Figure 6: A depiction of the flows corresponding to figure 3b, for which  $\theta_{b_1} = 60$  and  $\theta_{b_2} = 0 \dots 200$ . Other labelling is as on figure 5.

We remarked while discussing figure 3 that the  $g$ -function plots stabilise as  $\theta_{b_1}$  increases. The same feature can be seen on comparing figure 5 with the equivalent diagram for  $\theta_{b_1} = 60$ , figure 6. For  $\mathcal{M}_3$  and  $\mathcal{M}_4$  the boundary conditions and flows appearing in figure 6 match those in figure 5, but for the higher minimal models the boundary conditions appearing are different. This corresponds to how the plots in figures 3b and 3d coincide for  $\ln r > -60$ .

#### 4 Exact $g$ -functions for $\mathcal{M}A_m^{(+)}$

Finally, we are ready to obtain the effective equations which govern the  $g$ -function flows for the boundary versions of the bulk interpolating theories  $\mathcal{M}A_m^{(+)}$ . These theories can be thought of as bulk perturbations of the minimal models  $\mathcal{M}_m$  by their  $\phi_{13}$  operators, with the sign of the perturbation chosen so that the infrared limit of the model is  $\mathcal{M}_{m-1}$ , the next minimal model

down. Our predictions for the associated boundary flows can be read from the results of the last section, but to obtain exact equations, we need to take a careful limit of the  $g$ -function formula in parallel with the double-scaling limit of the bulk TBA equations.

To fix notations we first review the situation for the bulk TBA. The TBA system proposed in [16] for  $\mathcal{MA}_m^{(+)}$  involves  $m - 2$  pseudoenergies  $\epsilon_1 \dots \epsilon_{m-2}$ , coupled together by the following system of TBA equations:

$$\begin{aligned}\epsilon_1(\theta) &= \frac{1}{2}\hat{r}e^\theta - \int_{\mathbb{R}} \phi(\theta - \theta')L_2(\theta') d\theta' \\ \epsilon_a(\theta) &= - \int_{\mathbb{R}} \phi(\theta - \theta')(L_{a-1}(\theta') + L_{a+1}(\theta')) d\theta' \quad a = 2 \dots m-3 \\ \epsilon_{m-2}(\theta) &= \frac{1}{2}\hat{r}e^{-\theta} - \int_{\mathbb{R}} \phi(\theta - \theta')L_{m-1}(\theta') d\theta'\end{aligned}\tag{4.1}$$

where  $L_a(\theta) = \ln(1 + e^{-\epsilon_a(\theta)})$ ,  $\phi(\theta) = 1/(2\pi \cosh(\theta))$  is as in (2.6), and  $\hat{r}$  sets the crossover scale. The effective central charge is then

$$c_{\text{eff}}(\hat{r}) = \frac{3\hat{r}}{2\pi^2} \int_{\mathbb{R}} (e^\theta L_1(\theta) + e^{-\theta} L_{m-2}(\theta)) d\theta\tag{4.2}$$

and as  $\ln(\hat{r})$  increases through a region of size of order 1 about the origin,  $c_{\text{eff}}(\hat{r})$  moves from  $c_m$  to  $c_{m-1}$ , consistent with the corresponding bulk flow being from  $\mathcal{M}_m$  to  $\mathcal{M}_{m-1}$ .

These same equations emerge from a double-scaling limit of the staircase model if we set

$$\ln(r) = -(m-3)\theta_0/2 + \ln(\hat{r})\tag{4.3}$$

and then take the limit  $\theta_0 \rightarrow \infty$  keeping  $\ln(\hat{r})$  finite, before finally allowing  $\ln(\hat{r})$  to vary from  $-\infty$  to  $+\infty$ . In particular, the pseudoenergies  $\epsilon_a(\theta)$  are recovered from the staircase pseudoenergy  $\epsilon(\theta)$  in the  $\theta_0 \rightarrow \infty$  limit by setting

$$\epsilon_a(\theta) = \epsilon(\theta + (m-1-2a)\theta_0/2), \quad a = 1 \dots m-2\tag{4.4}$$

and only allowing  $\theta$  to vary over the full real line after the limit has been taken.

It turns out that in this limit the staircase  $g$ -function formulae can be rewritten in terms of the limiting pseudoenergies  $\epsilon_a(\theta)$  and various constants which can be calculated in terms of the plateau values of the staircase pseudoenergies. We start with the infinite series part of the  $g$ -function, (2.13). Crucial to the analysis is the double-bump shape of the kernel  $\phi_S(\theta)$ , shown in figure 1, which causes each multiple integral contributing to the sum to localise onto a collection of subregions of  $\mathbb{R}^n$ . In each of these subregions, the staircase pseudoenergy is either constant, or else is uniformly well-approximated by one of the interpolating-flow pseudoenergies  $\epsilon_a(\theta)$ . Rewriting the formula for  $\ln g_0$  in terms of these constants and functions leads to the effective equations which govern the  $g$ -function flow in  $\mathcal{MA}_m^{(+)}$ .

More precisely, since  $\phi_S(\theta) = \phi(\theta - \theta_0) + \phi(\theta + \theta_0)$ , each term  $\phi_S(\theta_1 + \theta_2)\phi_S(\theta_2 - \theta_3) \dots \phi_S(\theta_n - \theta_1)$  in the sum in (2.13) can be expanded as sum of  $2^n$  terms of the form

$$\phi(\theta_1 + \theta_2 - \alpha_1\theta_0)\phi(\theta_2 - \theta_3 - \alpha_2\theta_0) \dots \phi(\theta_n - \theta_1 - \alpha_n\theta_0)\tag{4.5}$$

where each  $\alpha_k = \pm 1$ . The decay properties of  $\phi(\theta)$  mean that it is only non-zero for  $\theta \approx 0$ , so for the above term to be non-zero as  $\theta_0 \rightarrow \infty$  we require

$$\begin{aligned}\theta_1 + \theta_2 &\approx \alpha_1\theta_0 \\ \theta_2 - \theta_3 &\approx \alpha_2\theta_0 \\ &\vdots \\ \theta_n - \theta_1 &\approx \alpha_n\theta_0\end{aligned}\tag{4.6}$$



from which it follows that  $\theta_k \approx \bar{\theta}_k$ ,  $k = 1 \dots n$ , where

$$\begin{pmatrix} \bar{\theta}_2 \\ \bar{\theta}_3 \\ \cdot \\ \cdot \\ \bar{\theta}_n \\ \bar{\theta}_1 \end{pmatrix} = \frac{1}{2}\theta_0 \begin{pmatrix} 1 & 1 & 1 & 1 & \cdots & 1 \\ 1 & -1 & 1 & 1 & \cdots & 1 \\ 1 & -1 & -1 & 1 & \cdots & 1 \\ \cdot & \cdot & \cdot & \cdot & \cdot & \cdot \\ \cdot & \cdot & \cdot & \cdot & \cdot & \cdot \\ 1 & -1 & -1 & -1 & \cdots & -1 \end{pmatrix} \begin{pmatrix} \alpha_1 \\ \alpha_2 \\ \cdot \\ \cdot \\ \cdot \\ \alpha_n \end{pmatrix}. \quad (4.7)$$

and the integral over  $\mathbb{R}^n$  has indeed localised, to a set of  $2^n$  regions of size of order one as  $\theta_0 \rightarrow \infty$ , which become infinitely separated in this limit. The coordinates  $\bar{\theta}_k$  of the centres of these regions are either all even multiples of  $\theta_0/2$ , or all odd multiples of  $\theta_0/2$ , depending on whether  $n$  is even or odd.

For each region of integration we must consider the behaviours of the ‘measure factors’  $1/(1 + e^{\epsilon(\theta_k)})$ ,  $k = 1 \dots n$ . As for the function  $L(\theta)$  discussed above, these factors exhibit a series of plateaux interleaved by transition regions, at  $\theta \approx \theta_a \equiv (m-1-2a)\theta_0/2$ ,  $a = 1 \dots m-2$ . Within these transition regions, the measure factors are well-approximated in the  $\theta_0 \rightarrow \infty$  limit by the functions  $1/(1 + e^{\epsilon_a})$ , by (4.4). In between these regions the measure factors are approximately constant, and can be expressed in terms of the numbers  $y_a|_{\mathcal{M}_m} = x_a|_{\mathcal{M}_{m-1}}$ ,  $a = 1 \dots m-1$ . Taking these considerations into account, the terms in the sum in (2.13) fall into two categories:

- (a) If  $m+n$  is odd, every  $\bar{\theta}_k$  satisfying  $|\bar{\theta}_k| \leq (m-3)\theta/2$  lies in a transition region for  $\epsilon(\theta)$ , so that its measure factor remains nontrivial even after the  $\theta_0 \rightarrow \infty$  limit has been taken. We denote the part of  $\ln g_0$  consisting of these these terms by  $\ln g_A(\hat{r})$ .
- (b) If  $m+n$  is even, every  $\bar{\theta}_k$  lies inside a plateau of  $\epsilon(\theta)$  after the  $\theta_0 \rightarrow \infty$  limit has been taken, so that the corresponding measure factor becomes constant. We denote the ( $\hat{r}$ -independent) part of  $\ln g_0$  consisting of these these terms by  $\ln g_B$ .

For the (a) terms, the values of  $\epsilon(\theta \approx \bar{\theta}_k)$  vary as  $\hat{r}$  varies, and only reach plateau values in the UV and IR limits, these values being  $x_{k+1}|_{\mathcal{M}_m}$  in the UV and  $y_k|_{\mathcal{M}_{m-1}}$  in the IR. Rewriting the formulae in each subregion of integration in terms of the limiting pseudoenergies  $\epsilon_a(\theta)$  using (4.4) and shifting the integration variables to remove all appearances of  $\theta_0$ , we found that  $\ln g_A$  can be rewritten in the  $\theta_0 \rightarrow \infty$ ,  $\hat{r}$  finite limit as

$$\ln g_A(\hat{r}) = \sum_{\substack{n \geq 1 \\ m+n \text{ odd}}} \frac{1}{2n} \int_{\mathbb{R}^n} \text{antiTr}(\Pi_{i=1}^n A(\theta_i) d\theta_i) \phi(\theta_1 - \theta_2) \phi(\theta_2 - \theta_3) \cdots \phi(\theta_{n-1} - \theta_n) \phi(\theta_n + \theta_1) \quad (4.8)$$

where the  $(m-2) \times (m-2)$  matrix  $A(\theta)$  is given by

$$A(\theta) = \begin{pmatrix} 0 & \frac{1}{1+e^{\epsilon_1(\theta)}} & 0 & 0 & \cdots & 0 & 0 & 0 \\ \frac{1}{1+e^{\epsilon_2(\theta)}} & 0 & \frac{1}{1+e^{\epsilon_2(\theta)}} & 0 & \cdots & 0 & 0 & 0 \\ 0 & \frac{1}{1+e^{\epsilon_3(\theta)}} & 0 & \frac{1}{1+e^{\epsilon_3(\theta)}} & \cdots & 0 & 0 & 0 \\ \vdots & \vdots & \vdots & \vdots & \vdots & \vdots & \vdots & \vdots \\ 0 & 0 & 0 & 0 & \cdots & \frac{1}{1+e^{\epsilon_{m-3}(\theta)}} & 0 & \frac{1}{1+e^{\epsilon_{m-3}(\theta)}} \\ 0 & 0 & 0 & 0 & \cdots & 0 & \frac{1}{1+e^{\epsilon_{m-2}(\theta)}} & 0 \end{pmatrix} \quad (4.9)$$

and  $\text{antiTr}(K)$ , the anti-trace of an  $M \times M$  matrix  $K$ , is defined as the sum of its anti-diagonal elements, or equivalently

$$\text{antiTr}(K) = \text{Tr}(KJ), \quad \text{where } J_{ij} = \delta_{i, M+1-j}. \quad (4.10)$$

The measure factors for the (b) terms are by contrast constant throughout the relevant integration subregions. They can therefore be pulled outside their integrals, leaving only the various factors of  $\phi(\theta)$ . This leads to the following expression for  $\ln g_B$ :

$$\begin{aligned} \ln g_B &= \sum_{\substack{n \geq 1 \\ m+n \text{ even}}} \frac{1}{2n} \text{antiTr}(B^n) \int_{\mathbb{R}^n} \phi(\theta_1 - \theta_2) \phi(\theta_2 - \theta_3) \cdots \phi(\theta_{n-1} - \theta_n) \phi(\theta_n + \theta_1) d\theta_1 \cdots d\theta_n \\ &= \sum_{\substack{n \geq 1 \\ m+n \text{ even}}} \frac{1}{n2^{n+2}} \text{antiTr}(B^n) = \sum_{\substack{n \geq 1 \\ m+n \text{ even}}} \frac{1}{n2^{n+2}} \text{Tr}(B^n J) \end{aligned} \quad (4.11)$$

where the tridiagonal  $(m-3) \times (m-3)$  matrix  $B$  is equal to the limit as  $\theta_0 \rightarrow \infty$  of

$$\begin{pmatrix} 0 & \frac{1}{1+e^{\epsilon(\frac{m-4}{2}\theta_0)}} & 0 & \cdots & 0 & 0 & 0 \\ \frac{1}{1+e^{\epsilon(\frac{m-6}{2}\theta_0)}} & 0 & \frac{1}{1+e^{\epsilon(\frac{m-6}{2}\theta_0)}} & \cdots & 0 & 0 & 0 \\ 0 & \frac{1}{1+e^{\epsilon(\frac{m-8}{2}\theta_0)}} & 0 & \cdots & 0 & 0 & 0 \\ \vdots & \vdots & \vdots & & \vdots & \vdots & \vdots \\ 0 & 0 & 0 & \cdots & \frac{1}{1+e^{\epsilon(-\frac{m-6}{2}\theta_0)}} & 0 & \frac{1}{1+e^{\epsilon(-\frac{m-6}{2}\theta_0)}} \\ 0 & 0 & 0 & \cdots & 0 & \frac{1}{1+e^{\epsilon(-\frac{m-4}{2}\theta_0)}} & 0 \end{pmatrix}$$

The explicit form of this matrix can be found using the  $L(\theta)$  plateau values (3.11) and is

$$\begin{pmatrix} 0 & 1 - \frac{\sin^2 \frac{\pi}{m}}{\sin^2 \frac{2\pi}{m}} & 0 & \cdots & 0 & 0 & 0 \\ 1 - \frac{\sin^2 \frac{\pi}{m}}{\sin^2 \frac{3\pi}{m}} & 0 & 1 - \frac{\sin^2 \frac{\pi}{m}}{\sin^2 \frac{3\pi}{m}} & \cdots & 0 & 0 & 0 \\ 0 & 1 - \frac{\sin^2 \frac{\pi}{m}}{\sin^2 \frac{4\pi}{m}} & 0 & \cdots & 0 & 0 & 0 \\ \vdots & \vdots & \vdots & & \vdots & \vdots & \vdots \\ 0 & 0 & 0 & \cdots & 1 - \frac{\sin^2 \frac{\pi}{m}}{\sin^2 \frac{(m-3)\pi}{m}} & 0 & 1 - \frac{\sin^2 \frac{\pi}{m}}{\sin^2 \frac{(m-3)\pi}{m}} \\ 0 & 0 & 0 & \cdots & 0 & 1 - \frac{\sin^2 \frac{\pi}{m}}{\sin^2 \frac{(m-2)\pi}{m}} & 0 \end{pmatrix}$$

or, more concisely,

$$B_{ab} = l_{ab} x_{a+1} / (1 + x_{a+1}) \quad (4.12)$$

where  $x_a = x_a|_{\mathcal{M}_{m-1}} = \frac{\sin^2(\pi a/m)}{\sin^2(\pi/m)} - 1$ , and  $l_{ab}$  is the incidence matrix of the  $A_{m-3}$  Dynkin diagram. Note that  $B$  is the transpose of a matrix which arises in the analysis of small fluctuations about stationary solutions of an associated Y-system [16] and has eigenvalues

$$\lambda_k = 2 \cos\left(\frac{\pi k}{m}\right), \quad k = 2, 3, \dots, m-2. \quad (4.13)$$

For later use we note that  $[B, J] = 0$ , and furthermore that the eigenvector  $\psi_k$  of  $B$  corresponding to the eigenvalue  $\lambda_k$  satisfies

$$J\psi_k = (-1)^k \psi_k. \quad (4.14)$$

As explained in appendix A, this information is enough to evaluate (4.11) in closed form,

with the result

$$\ln g_B|_{\mathcal{M}A_m^{(+)}} = \begin{cases} \ln \left( \left( \frac{4}{m} \right)^{\frac{1}{4}} \frac{\sin \frac{(m-1)\pi}{2m}}{\sqrt{\sin \frac{\pi}{m}}} \right) & \text{for } m \text{ odd} \\ \ln \left( \left( \frac{2}{m} \right)^{\frac{1}{4}} \frac{1}{\sqrt{\sin \frac{\pi}{m}}} \right) & \text{for } m \text{ even} . \end{cases} \quad (4.15)$$

$$\ln \left( \left( \frac{2}{m} \right)^{\frac{1}{4}} \frac{1}{\sqrt{\sin \frac{\pi}{m}}} \right) \quad \text{for } m \text{ even} . \quad (4.16)$$

A missing piece of the staircase discussion from the previous section can now be filled in, namely the formulae (3.12) and (3.13) for the value of  $\ln g_0|_{\mathcal{M}_m}$  when the bulk staircase theory is in the vicinity of  $\mathcal{M}_m$ . In terms of the limiting  $g$ -function equations for  $\mathcal{M}A_m^{(+)}$ , this number is equal to the UV limit of  $\ln g_A(\hat{r}) + \ln g_B$  as  $\hat{r} \rightarrow 0$ . Considering the limiting forms of the matrix  $A(\theta)$ , given by (4.9), as  $\hat{r} \rightarrow 0$ , it is straightforwardly seen that

$$\ln g_A(0)|_{\mathcal{M}A_m^{(+)}} = \ln g_B|_{\mathcal{M}A_{m+1}^{(+)}} \quad (4.17)$$

and so

$$\ln g_0|_{\mathcal{M}_m} = \ln g_B|_{\mathcal{M}A_{m+1}^{(+)}} + \ln g_B|_{\mathcal{M}A_m^{(+)}} \quad (4.18)$$

which, via (4.15) and (4.16), leads immediately to (3.12) and (3.13).

The remainder of the exact  $g$ -function,  $\ln g_b = \ln g_{b1} + \ln g_{b2} + \ln g_{b3}$ , is more straightforward to analyse. In the limit  $\{\theta_0 \rightarrow \infty, \ln \hat{r} \text{ finite}\}$ , the behaviours of the first two terms,  $\ln g_{b1}$  and  $\ln g_{b2}$ , depend on whether  $m$  is even or odd.

The presence of  $\phi(\theta)$  and  $\delta(\theta)$  in the expression (3.1) for  $\ln g_{b1}$  means that this term is determined by the staircase pseudoenergy close to  $\theta = 0$ . When  $m$  is odd this remains nontrivial as the double-scaling limit is taken and, using the pseudoenergies defined in (4.4),  $\ln g_{b1}$  becomes

$$\ln g_{b1} = -\frac{1}{2} \int_{\mathbb{R}} d\theta \left( \phi(\theta) + \frac{1}{2} \delta(\theta) \right) \ln(1 + e^{-\epsilon \frac{m-1}{2}(\theta)}), \quad (4.19)$$

which has UV and IR limits given by (3.14) at  $\mathcal{M}_m$  and (3.15) at  $\mathcal{M}_{m-1}$  respectively. When  $m$  is even, the staircase pseudoenergy instead becomes constant near to  $\theta = 0$ , giving

$$\ln g_{b1} = -\frac{1}{2} \ln(1 + y_{m/2}|_{\mathcal{M}_m}) \quad (4.20)$$

matching (3.15) at  $\mathcal{M}_m$  and also (3.14) at  $\mathcal{M}_{m-1}$ .

In contrast, the formula (3.2) for  $\ln g_{b2}$  involves  $\phi_{(\frac{3}{4})}(\theta \pm \frac{1}{2}\theta_0)$  and  $\phi(2\theta \pm \theta_0)$ , meaning that  $\ln g_{b2}$  is determined by the behaviour of  $L(\theta)$  close to  $\theta = \pm\theta_0/2$ . For  $m$  odd, the limiting form of  $L(\theta \approx \pm\theta_0/2)$  is constant, and

$$\ln g_{b2} = -\frac{1}{2} \ln(1 + y_{\frac{m-1}{2}}|_{\mathcal{M}_m}) \quad (4.21)$$

as in (3.16) at  $\mathcal{M}_m$  and (3.17) at  $\mathcal{M}_{m-1}$ . When  $m$  is even,  $L(\theta \approx \pm\theta_0/2)$  remains nontrivial and in the limit

$$\ln g_{b2} = \int_{\mathbb{R}} d\theta \left( \phi_{(\frac{3}{4})}(\theta) - \phi(2\theta) \right) \ln(1 + e^{-\epsilon \frac{m-2}{2}(\theta)}), \quad (4.22)$$

with UV and IR limits given by (3.17) at  $\mathcal{M}_m$  and (3.16) at  $\mathcal{M}_{m-1}$  respectively.

To allow the last part of  $\ln g_b$ ,  $\ln g_{b3}$ , to retain a non-trivial  $\hat{r}$ -dependence in the limit, we pick two integers  $a_1$  and  $a_2$  with  $0 \leq a_i \leq m-1$ , write the boundary parameters  $\theta_{b1}$  and  $\theta_{b2}$  as

$$\theta_{b_i} = \frac{1}{2}(m-1-2a_i)\theta_0 + \hat{\theta}_{b_i} \quad (4.23)$$

for  $i = 1, 2$ , and then take the  $\theta_0 \rightarrow \infty$  limit keeping  $\hat{\theta}_{b1}$  and  $\hat{\theta}_{b2}$  finite. Given the specification (4.4) of the effective pseudoenergies  $\epsilon_a(\theta)$ , for  $1 \leq a_i \leq m-2$  the staircase expression (3.3) for  $\ln g_{b3}$  then reduces to

$$\begin{aligned} \ln g_{b3 \ a_1 a_2}(\hat{r}, \hat{\theta}_{b1}, \hat{\theta}_{b2}) &= \frac{1}{2} \sum_{i=1}^2 \int_{\mathbb{R}} d\theta (\phi(\theta - \hat{\theta}_{b_i}) + \phi(\theta + \hat{\theta}_{b_i})) \ln(1 + e^{-\epsilon_{a_i}(\theta)}) \\ &= \sum_{i=1}^2 \int_{\mathbb{R}} d\theta \phi(\theta - \hat{\theta}_{b_i}) \ln(1 + e^{-\epsilon_{a_i}(\theta)}) \end{aligned} \quad (4.24)$$

where the symmetry  $\epsilon_a(\theta) = \epsilon_{m-1-a}(-\theta)$  of the ground-state pseudoenergies for  $\mathcal{MA}_m^{(+)}$  was used in going from the first line to the second. If either  $a_i$  is equal to 0 or  $m-1$ , then the staircase pseudoenergy diverges in the region of  $\theta_{b_i}$ , and the corresponding term in (4.24) is zero in the  $\mathcal{MA}_m^{(+)}$  limit.

To summarize the results of this section, our final expressions for the two-parameter families of exact  $g$ -functions for  $\mathcal{MA}_m^{(+)}$ , indexed by a pair of integers  $a_1$  and  $a_2$  and expressed in terms of the rescaled variables  $\hat{r}$ ,  $\hat{\theta}_{b1}$  and  $\hat{\theta}_{b2}$ , are as follows:

- $m$  odd:

$$\begin{aligned} \ln g_{a_1 a_2}(\hat{r}, \hat{\theta}_{b1}, \hat{\theta}_{b2}) &= \ln \left( \left( \frac{4}{m} \right)^{\frac{1}{4}} \sqrt{\sin \frac{\pi}{m}} \right) - \frac{1}{2} \int_{\mathbb{R}} d\theta (\phi(\theta) + \frac{1}{2} \delta(\theta)) \ln(1 + e^{-\epsilon_{\frac{m-1}{2}}(\theta)}) \\ &\quad + \ln g_A(\hat{r}) + \ln g_{b3 \ a_1 a_2}(\hat{r}, \hat{\theta}_{b1}, \hat{\theta}_{b2}); \end{aligned} \quad (4.25)$$

- $m$  even:

$$\begin{aligned} \ln g_{a_1 a_2}(\hat{r}, \hat{\theta}_{b1}, \hat{\theta}_{b2}) &= \ln \left( \left( \frac{2}{m} \right)^{\frac{1}{4}} \sqrt{\sin \frac{\pi}{m}} \right) + \int_{\mathbb{R}} d\theta (\phi_{(\frac{3}{4})}(\theta) - \phi(2\theta)) \ln(1 + e^{-\epsilon_{\frac{m-2}{2}}(\theta)}) \\ &\quad + \ln g_A(\hat{r}) + \ln g_{b3 \ a_1 a_2}(\hat{r}, \hat{\theta}_{b1}, \hat{\theta}_{b2}). \end{aligned} \quad (4.26)$$

In both cases  $g_A$  is given by (4.8), the sum over  $n$  running through even integers for  $m$  odd, and odd integers for  $m$  even, with the pseudoenergies involved solving the bulk  $\mathcal{MA}_m^{(+)}$  TBA system (4.1). The term  $g_{b3 \ a_1 a_2}$  is as defined in (4.24). The constant terms result from adding  $\ln g_B$ , given by (4.15) or (4.16), to  $\ln g_{b2}$  for  $m$  odd, and to  $\ln g_{b1}$  for  $m$  even. The remaining integral term is  $\ln g_{b1}$  for  $m$  odd and  $\ln g_{b2}$  for  $m$  even. Formally setting one or both of  $a_1$  and  $a_2$  equal to 0 or  $m-1$ , as discussed after (4.24), incorporates the limiting one- and zero- parameter families of flows found by deleting the  $\hat{\theta}_{b1}$  and/or  $\hat{\theta}_{b2}$  dependent parts of  $\ln g_{b3}$ . If both are deleted so that  $\ln g_{b3}$  is identically zero, then by the results of the last section the  $g$ -function flow should be from  $g(m, 1, 1)$  at  $\hat{r} = 0$  to  $g(m-1, 1, 1)$  as  $\hat{r} \rightarrow \infty$ . This can be checked directly. Simplest is the UV limit. For  $m$  odd, using (3.14) and (4.17), the first three terms on the RHS of (4.25) tend to

$$\ln \left( \left( \frac{4}{m} \right)^{\frac{1}{4}} \sqrt{\sin \frac{\pi}{m}} \right) - \frac{1}{2} \ln \left( \frac{1}{\sin^2 \left( \frac{\pi}{m+1} \right)} \right) + \ln \left( \left( \frac{2}{m+1} \right)^{\frac{1}{4}} \frac{1}{\sqrt{\sin \frac{\pi}{m+1}}} \right) \quad (4.27)$$

which is equal to  $g(m, 1, 1)$ . Similarly, for  $m$  even, (3.17) and (4.17) imply that the first three terms on the RHS of (4.26) become

$$\ln \left( \left( \frac{2}{m} \right)^{\frac{1}{4}} \sqrt{\sin \frac{\pi}{m}} \right) - \frac{1}{2} \ln \left( \frac{\sin^2 \left( \frac{\pi m}{2(m+1)} \right)}{\sin^2 \left( \frac{\pi}{m+1} \right)} \right) + \ln \left( \left( \frac{4}{m+1} \right)^{\frac{1}{4}} \frac{\sin \left( \frac{m\pi}{2(m+1)} \right)}{\sqrt{\sin \frac{\pi}{m+1}}} \right) \quad (4.28)$$

and the value of  $g(m, 1, 1)$  is again reproduced.

In the  $\hat{r} \rightarrow \infty$ , IR, limit the matrix  $A(\theta_i)$  defined in (4.9) again becomes independent of  $\theta$  in the central region  $\theta \approx 0$  where the integrals in (4.8) have their support, and tends to the following  $(m-2) \times (m-2)$  matrix:

$$A_{\text{IR}} = \begin{pmatrix} 0 & 0 & 0 & \cdots & 0 & 0 & 0 \\ 1 - \frac{\sin^2 \frac{\pi}{m-1}}{\sin^2 \frac{2\pi}{m-1}} & 0 & 1 - \frac{\sin^2 \frac{\pi}{m-1}}{\sin^2 \frac{2\pi}{m-1}} & \cdots & 0 & 0 & 0 \\ 0 & 1 - \frac{\sin^2 \frac{\pi}{m-1}}{\sin^2 \frac{3\pi}{m-1}} & 0 & \cdots & 0 & 0 & 0 \\ \vdots & \vdots & \vdots & & \vdots & \vdots & \vdots \\ 0 & 0 & 0 & \cdots & 1 - \frac{\sin^2 \frac{\pi}{m-1}}{\sin^2 \frac{(m-3)\pi}{m-1}} & 0 & 1 - \frac{\sin^2 \frac{\pi}{m-1}}{\sin^2 \frac{(m-3)\pi}{m-1}} \\ 0 & 0 & 0 & \cdots & 0 & 0 & 0 \end{pmatrix}. \quad (4.29)$$

In terms of  $A_{\text{IR}}$ ,

$$\ln g_A(\infty) = \sum_{\substack{n \geq 1 \\ m+n \text{ odd}}} \frac{1}{n2^{n+2}} \text{Tr}((A_{\text{IR}})^n J). \quad (4.30)$$

To evaluate this sum, observe that the central  $(m-4) \times (m-4)$  sub-matrix of  $A_{\text{IR}}$  is the matrix  $B$  for  $\mathcal{MA}_{m-1}^{(+)}$ . Furthermore, the zero values of all entries in the first and final rows means that the central  $(m-4) \times (m-4)$  sub-matrix of  $(A_{\text{IR}})^n$  is just  $(B|_{\mathcal{MA}_{m-1}^{(+)}})^n$ , and the entries on the first and final rows are again zero. Hence the traces and antitraces of  $(A_{\text{IR}})^n$  are equal to those of  $(B|_{\mathcal{MA}_{m-1}^{(+)}})^n$ , and

$$\ln g_{0_A}(\infty)|_{\mathcal{MA}_m^{(+)}} = \ln g_{0_B}|_{\mathcal{MA}_{m-1}^{(+)}} \quad (4.31)$$

allowing (4.15) and (4.16) at  $m-1$  to be used to compute  $\ln g_{0_A}(\infty)|_{\mathcal{MA}_m^{(+)}}$ . For  $m$  odd, using (3.15) and (4.16) at  $m-1$ , the first three terms of (4.25) therefore become

$$\ln \left( \left( \frac{4}{m} \right)^{\frac{1}{4}} \sqrt{\sin \frac{\pi}{m}} \right) - \frac{1}{2} \ln \left( \frac{1}{\sin^2 \left( \frac{\pi}{m-1} \right)} \right) + \ln \left( \left( \frac{2}{m-1} \right)^{\frac{1}{4}} \frac{1}{\sqrt{\sin \frac{\pi}{m-1}}} \right)$$

which is indeed equal to  $g(m-1, 1, 1)$ . Similarly, for  $m$  even, in the  $\hat{r} \rightarrow \infty$  limit the first three terms of (4.26) are, by (3.16) and (4.15) at  $m-1$ ,

$$\ln \left( \left( \frac{2}{m} \right)^{\frac{1}{4}} \sqrt{\sin \frac{\pi}{m}} \right) - \frac{1}{2} \ln \left( \frac{\sin^2 \left( \frac{(m-2)\pi}{2(m-1)} \right)}{\sin^2 \left( \frac{\pi}{m-1} \right)} \right) + \ln \left( \left( \frac{4}{m-1} \right)^{\frac{1}{4}} \frac{\sin \left( \frac{(m-2)\pi}{2(m-1)} \right)}{\sqrt{\sin \frac{\pi}{m-1}}} \right) \quad (4.32)$$

which again matches  $g(m-1, 1, 1)$ .

More generally, the full equations (4.25) or (4.26) predict a collection of two-parameter families of flows, indexed by the two integers  $a_1$  and  $a_2$ . The relevant calculations have been carried out in the last section and we won't repeat them here. Instead, in figure 7 below we show a typical family of flows, where  $r = a_1 + 1$  and  $s = a_2 + 1$ . All flows for  $\hat{\theta}_{b_1}$  and  $\hat{\theta}_{b_2}$  finite start in the far UV at the  $[x_r, x_s]$  boundary of  $\mathcal{M}_m$ , a superposition of Cardy boundaries given by the rule (3.26). If both  $\hat{\theta}_{b_1}$  and  $\hat{\theta}_{b_2}$  are zero, the flow is directly downwards to the  $[y_{r-1}, y_{s-1}]$  boundary of  $\mathcal{M}_{m-1}$ , driven by the bulk perturbation. Nonzero values of  $\hat{\theta}_{b_1}$  and  $\hat{\theta}_{b_2}$  correspond to the addition of boundary perturbations to the bulk perturbation, and cause the trajectory to visit other boundaries on its way from UV to IR, as can be read from the figure. If either of  $a_1$  or  $a_2$  is equal to 1 or  $m-2$ , so that one or both of  $r$  and  $s$  is equal to 2 or  $m-1$ , the cube shown

in figure 7 truncates, the equalities  $x_1 = y_1$  or  $x_{m-1} = y_{m-2}$  within  $\mathcal{M}_{m-1}$  causing one or two rows on the bottom face of the cube to fuse together, resulting in the flow patterns illustrated in figure 8. The same phenomenon was seen earlier for the staircase model, and is reflected in the diagonal lines of flows running from top right to bottom left in figures 5 and 6.

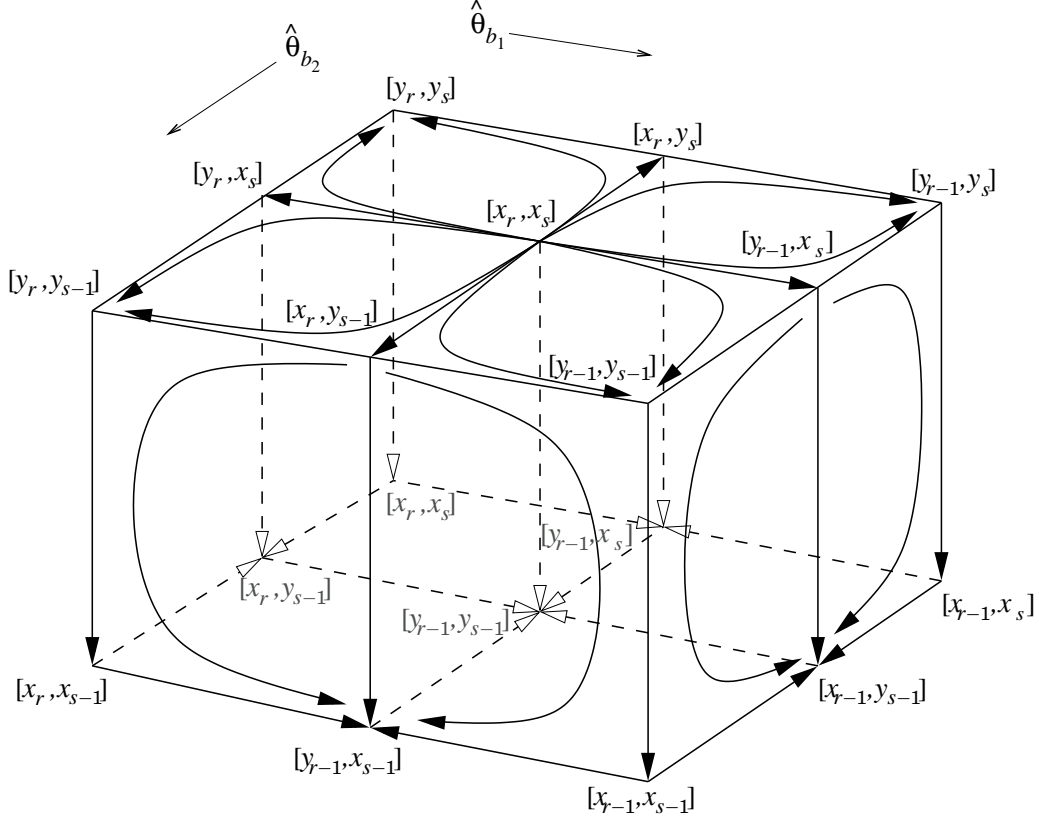


Figure 7: A cube of  $\mathcal{MA}_m^{(+)}$  flows, where  $r = a_1 + 1$  and  $s = a_2 + 1$ . Flows on the outer faces occur for  $\hat{\theta}_{b_1} \rightarrow \pm\infty$  and/or  $\hat{\theta}_{b_2} \rightarrow \pm\infty$ ; those on the top face are within the minimal model  $\mathcal{M}_m$ , and those on the bottom are within  $\mathcal{M}_{m-1}$ . The central vertical axis corresponds to  $\hat{\theta}_{b_1} = \hat{\theta}_{b_2} = 0$ . Conformal boundary conditions at fixed points of the flows are labelled according to the scheme given in equation (3.26).

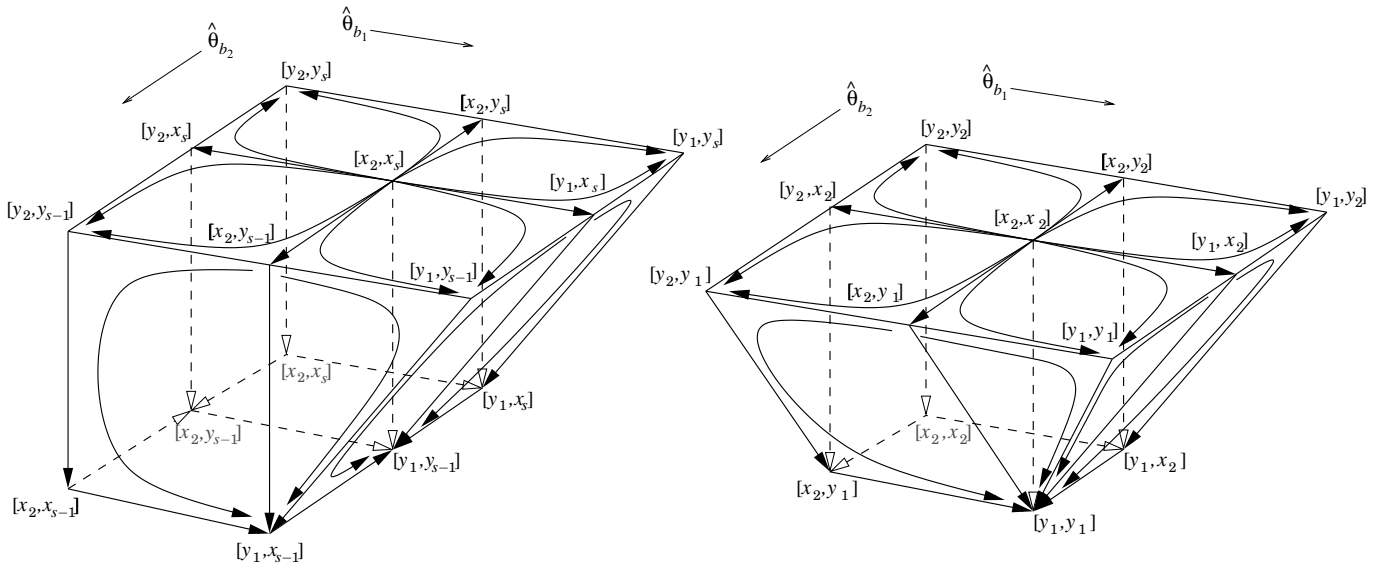


Figure 8: Truncations of the cube of flows for  $r = 2$  (left) and  $r = s = 2$  (right), corresponding to setting either  $a_1 = 1$  or  $a_1 = a_2 = 1$  in (4.24). Other details are as on figure 7.

## 5 Conclusions

In this paper we have shown how exact methods can be used to study interpolating boundary flows in two-dimensional integrable models in situations where both bulk and boundary are away from criticality. Our results for flows between minimal models have confirmed and extended previous perturbative studies. In addition we have shown how these flows can be embedded into larger manifolds of boundary integrability via the staircase model, generalising the picture seen in the bulk. In fact the staircase description is remarkably economical – the bulk S-matrix (2.1) and the boundary reflection factor (2.9) (or (2.11)) together encode not only all of the unitary  $c < 1$  minimal models, but also all of their Cardy boundary conditions and a variety of their superpositions, once fed into the general TBA and exact  $g$ -function machinery.

There are many directions for future work. Some perturbative checks of the exact equations for the tricritical to critical Ising bulk and boundary flows were undertaken in [5], but further tests higher up the series would be valuable, as would a more detailed study of the two-parameter boundary flows discussed in section 3, and their extensions via defects to incorporate further parameters through the more general reflection factor (2.11). The formulae found in section 4 describe, for the first time, exact off-critical  $g$ -functions in situations where the underlying scattering theory is non-diagonal, and it will be interesting to generalise the approach of Pozsgay [6] to cover such cases. At the same time, many other multiparameter families of integrable models with nontrivial intermediate scaling behaviours are now known, including generalisations of the staircase models [12–15], and the Homogeneous Sine-Gordon (HSG) models [30–32]. Hence there is plenty of scope to obtain more elaborate exact  $g$ -function flows using the approach adopted in this paper. Finally, it is noteworthy how the embedding of non-diagonal bulk and boundary scattering theories within higher-dimensional manifolds of integrability achieved by the staircase and HSG models manages to ‘abelianise’ their TBA descriptions. It would be very interesting to know how general this phenomenon is, and to understand it at a deeper level. At the very least, it demonstrates once again that simple exact S-matrices and reflection factors can hide a great deal of internal structure.

**Acknowledgements** – We would like to thank Peter Bowcock, Ed Corrigan, Matthias Gaberdiel, Balázs Pozsgay, Gabor Takacs and Gérard Watts for interesting and helpful discussions about this project, and, especially, Chaiho Rim for collaboration in its early stages. PED thanks the Perimeter Institute and the Centro de Ciencias de Benasque Pedro Pascual for hospitality. The work was supported in part by an STFC rolling grant, number ST/G000433/1, and by an STFC studentship (RMW).

## Appendix A Proofs of equations (4.15) and (4.16)

To derive (4.15) and (4.16) from (4.11), we first convert the final sum, over traces of products of powers of  $B$  with  $J$ , into a sum of traces of pure powers of related matrices, after which the identity

$$\sum_{n=1}^{\infty} \frac{1}{n} \text{Tr} M^n = -\text{Tr} \ln(I - M) = -\ln \text{Det}(I - M) \quad (\text{A.1})$$

will allow the sum to be evaluated in terms of the eigenvalues of these related matrices. There are two cases.

• If  $m$  is odd, then the sum in (4.11) is over odd powers of  $B$ . Shuffling indices and using the symmetries of  $B$  it can be checked that  $B^n J = (BJ)^n$  for all odd  $n$ , and so

$$\begin{aligned}\ln g_B &= \frac{1}{4} \text{Tr} \sum_{\substack{n \geq 1 \\ n \text{ odd}}} \frac{1}{n} \left(\frac{1}{2}BJ\right)^n \\ &= \frac{1}{8} \ln \frac{\text{Det} \left(1 + \frac{1}{2}BJ\right)}{\text{Det} \left(1 - \frac{1}{2}BJ\right)}.\end{aligned}\tag{A.2}$$

From (4.14), the eigenvalues of  $BJ$  are  $(-1)^k \lambda_k$ , which for  $m$  odd are the numbers  $2 \cos(2\pi/m)$ ,  $2 \cos(4\pi/m) \dots 2 \cos((m-3)\pi/m)$ , all with multiplicity two. Hence

$$\frac{\text{Det} \left(1 + \frac{1}{2}BJ\right)}{\text{Det} \left(1 - \frac{1}{2}BJ\right)} = \frac{\cos^4 \frac{\pi}{m} \cos^4 \frac{2\pi}{m} \dots \cos^4 \frac{(m-3)\pi}{2m}}{\sin^4 \frac{\pi}{m} \sin^4 \frac{2\pi}{m} \dots \sin^4 \frac{(m-3)\pi}{2m}}.\tag{A.3}$$

To evaluate this we call upon some well-known trigonometric identities. For the numerator we use

$$\cos \frac{\pi}{n} \cos \frac{2\pi}{n} \dots \cos \frac{(n-1)\pi}{2n} = \frac{1}{2^{(n-1)/2}} \quad \text{for } n \text{ odd}\tag{A.4}$$

and for the denominator

$$\sin \frac{\pi}{n} \sin \frac{2\pi}{n} \dots \sin \frac{(n-1)\pi}{n} = \frac{n}{2^{n-1}}\tag{A.5}$$

which implies

$$\sin^2 \frac{\pi}{n} \sin^2 \frac{2\pi}{n} \dots \sin^2 \frac{(n-1)\pi}{2n} = \frac{n}{2^{n-1}} \quad \text{for } n \text{ odd}.\tag{A.6}$$

Using (A.4) and (A.6),

$$\frac{\text{Det} \left(1 + \frac{1}{2}BJ\right)}{\text{Det} \left(1 - \frac{1}{2}BJ\right)} = \frac{1}{m^2} \frac{\sin^4 \frac{(m-1)\pi}{2m}}{\cos^4 \frac{(m-1)\pi}{2m}} = \left( \frac{4 \sin^4 \frac{(m-1)\pi}{2m}}{m \sin^2 \frac{\pi}{m}} \right)^2\tag{A.7}$$

and so (A.2) is in agreement with (4.15).

• If  $m$  is even, then the sum in (4.11) is instead over even powers of  $B$ . This time we make use of the identity, valid for  $m$  even, that

$$\text{Tr}(B^n J) = \text{Tr}(B^n - B'^n)\tag{A.8}$$

where  $B'$  is the  $(m-3) \times (m-3)$  matrix which only differs from  $B$  in the following elements:

$$B'_{\frac{m-2}{2}, \frac{m-4}{2}} = B'_{\frac{m-2}{2}, \frac{m}{2}} = 0.\tag{A.9}$$

To prove this identity we write the LHS as

$$\text{Tr}(B^n J) = B_{i_1 i_2} B_{i_2 i_3} \dots B_{i_{n-1} i_n} B_{i_n, m-i_1-2}\tag{A.10}$$

and note the following properties of  $B$ :

$$B_{i, i-1} = B_{i, i+1}, \quad \text{all other entries } 0;\tag{A.11}$$

$$B_{ij} = B_{m-2-i, m-2-j}.\tag{A.12}$$

The first of these means that (A.10) can be interpreted as a weighted sum over all  $n$ -step paths on the  $A_{m-3}$  Dynkin diagram which start and finish at pairs of conjugate nodes  $i_1$  and  $m-2-i_1$ ,  $i_1 = 1 \dots m-3$ , and move by one link at each step. Likewise  $\text{Tr}(B^n)$  and  $\text{Tr}(B'^n)$  are weighted



sums over  $n$ -step paths on the same Dynkin diagram, but which this time start and finish at the same node  $i_1$ , where again  $i_1$  is summed from 1 to  $m-3$ .

These observations imply that both sides of (A.10) are zero for  $n$  odd, and so from now on we can take  $n$  to be even (which is the case of direct interest in the current context). Due again to (A.11), a term in  $\text{Tr}(B^n J)$  with  $i_1 < \frac{m-2}{2}$  must include the element  $B_{\frac{m-2}{2} \frac{m}{2}}$ , and a term with  $i_1 > \frac{m-2}{2}$  must include the element  $B_{\frac{m-2}{2} \frac{m-4}{2}}$ . Assume first that  $i_1 < \frac{m-2}{2}$ , and consider

$$B_{i_1 i_2} B_{i_2 i_3} \cdots B_{i_{n-1} i_n} B_{i_n, m-2-i_1} \quad (\text{A.13})$$

for some particular  $i_2 \dots i_n$ . Suppose  $B_{\frac{m-2}{2} \frac{m}{2}}$  appears for the final time at  $B_{i_p i_{p+1}}$ , which means that  $B_{i_{p+1} i_{p+2}} = B_{\frac{m}{2} \frac{m+2}{2}}$ . By (A.12), the value of (A.13) is unchanged if all indices  $i_q$  with  $q > p$  are replaced by their conjugates  $m-2-i_q$ . The resulting term appears in the trace not of  $B^n J$ , but of  $B^n$ . Similarly, every term in the expansion of  $\text{Tr}(B^n J)$  with  $i_1 > \frac{m-2}{2}$  can be equated with a term in the expansion of  $\text{Tr}(B^n)$  with  $i_1 > \frac{m-2}{2}$ . Finally, the terms in the expansions of  $\text{Tr}(B^n J)$  and  $\text{Tr}(B^n)$  with  $i_1 = \frac{m-2}{2}$  are already equal, since  $i_1$  is then equal to  $m-2-i_1$ . Thus  $\text{Tr}(B^n J)$  is equal to the sum of the terms in the trace of  $B^n$  that include either  $B_{\frac{m-2}{2} \frac{m}{2}}$  or  $B_{\frac{m-2}{2} \frac{m-4}{2}}$  at least once. Now the trace of  $B^n$  as defined by (A.9) is equal to the trace of  $B^n$  minus the terms where  $B_{\frac{m-2}{2} \frac{m}{2}}$  or  $B_{\frac{m-2}{2} \frac{m-4}{2}}$  appears at least once. Hence  $\text{Tr}(B^n - B'^n)$  gives the required terms and (A.8) holds.

If  $m$  is even we therefore have

$$\begin{aligned} \ln g_B &= \sum_{\substack{n>1 \\ n \text{ even}}} \frac{1}{n 2^{n+2}} \text{Tr}(B^n J) \\ &= \frac{1}{4} \sum_{\substack{n>1 \\ n \text{ even}}} \frac{1}{n} \text{Tr} \left( \left(\frac{1}{2}B\right)^n - \left(\frac{1}{2}B'\right)^n \right) \\ &= \frac{1}{8} \ln \frac{\text{Det} \left( I - \frac{1}{4}(B')^2 \right)}{\text{Det} \left( I - \frac{1}{4}B^2 \right)} \end{aligned} \quad (\text{A.14})$$

using (A.1). To find the eigenvalues of  $B'$ ,  $\text{Det}(B' - \lambda I)$  can be expanded about the middle row to see that the characteristic polynomial of  $B'$  is proportional to  $\lambda$  times the product of the (equal) characteristic polynomials of the upper-left and lower-right  $(m-4)/2 \times (m-4)/2$  submatrices of  $B'$ , which we denote  $B'_1$  and  $B'_2$ . These submatrices can be fully diagonalised using the  $(m-4)/2$  eigenvectors  $\psi_k$  of  $B$  with  $k$  odd: from (4.14), these eigenvectors satisfy  $J\psi_k = -\psi_k$ . Hence their middle components are zero, while the neighbouring two are the negatives of each other. Given the definition (A.9) of  $B'$  this means that projecting each  $\psi_k$  for  $k$  odd onto its first  $(m-4)/2$  components yields  $(m-4)/2$  independent eigenvectors of  $B'_1$  with eigenvalues  $\lambda_k$ , and likewise for  $B'_2$ . Hence the eigenvalues of  $B'$  are

$$\lambda_k = 2 \cos\left(\frac{\pi k}{m}\right), \quad k = 3, 5 \dots m-3, \quad (\text{A.15})$$

each with multiplicity 2, together with 0. If  $m = 2 \pmod{4}$ , then 0 is also in the set (A.15), and so the algebraic multiplicity of the zero eigenvalue is 3, even though its geometric multiplicity turns out to be only 2. However, this lack of full diagonalisability makes no difference to the computations of traces.

We can now calculate  $\ln g_B$ . Evaluating (A.14) using the eigenvalues just obtained,

$$\begin{aligned} \frac{\text{Det} \left( I - \frac{1}{4}(B')^2 \right)}{\text{Det} \left( I - \frac{1}{4}B^2 \right)} &= \frac{\sin^4 \frac{3\pi}{m} \sin^4 \frac{5\pi}{m} \cdots \sin^4 \frac{(m-3)\pi}{m}}{\sin^2 \frac{2\pi}{m} \sin^2 \frac{3\pi}{m} \cdots \sin^2 \frac{(m-2)\pi}{m}} \\ &= \frac{\sin^2 \frac{3\pi}{m} \sin^2 \frac{5\pi}{m} \cdots \sin^2 \frac{(m-3)\pi}{m}}{\sin^2 \frac{2\pi}{m} \sin^2 \frac{4\pi}{m} \cdots \sin^2 \frac{(m-2)\pi}{m}}. \end{aligned} \quad (\text{A.16})$$

Labelling the final numerator  $X$  and the denominator  $Y$ , (A.5) at  $n = m$  and  $n = m/2$  respectively implies that

$$XY = \frac{1}{\sin^4 \frac{\pi}{m}} \left( \frac{m}{2^{m-1}} \right)^2, \quad Y = \frac{m^2}{2^m}. \quad (\text{A.17})$$

Hence

$$\frac{X}{Y} = \frac{\text{Det} \left( I - \frac{1}{4}(B')^2 \right)}{\text{Det} \left( I - \frac{1}{4}B^2 \right)} = \left( \frac{2}{m \sin^2 \frac{\pi}{m}} \right)^2 \quad (\text{A.18})$$

and (A.14) agrees with (4.16).

## References

- [1] P. Dorey, D. Fioravanti, C. Rim and R. Tateo, ‘Integrable quantum field theory with boundaries: The exact g-function’, Nucl. Phys. B **696** (2004) 445 [arXiv:hep-th/0404014].
- [2] P. Dorey, A. Lishman, C. Rim and R. Tateo, ‘Reflection factors and exact g-functions for purely elastic scattering theories’, Nucl. Phys. B **744** (2006) 239 [arXiv:hep-th/0512337].
- [3] A.M. Tsvetick, ‘The thermodynamics of the multichannel Kondo problem’, J. Phys. C **18** (1985) 159.
- [4] I. Affleck and A.W.W. Ludwig, ‘Universal noninteger ‘ground state degeneracy’ in critical quantum systems’, Phys. Rev. Lett. **67** (1991) 161.
- [5] P. Dorey, C. Rim and R. Tateo, ‘Exact g-function flow between conformal field theories’, Nucl. Phys. B **834** (2010) 485 [arXiv:0911.4969 [hep-th]].
- [6] B. Pozsgay, ‘On O(1) contributions to the free energy in Bethe Ansatz systems: the exact g-function’, arXiv:1003.5542 [hep-th].
- [7] F. Woyrnarovich, ‘On the normalization of the partition function of Bethe Ansatz systems’, arXiv:1007.1148 [cond-mat].
- [8] F. Lesage, H. Saleur and P. Simonetti, ‘Boundary flows in minimal models’, Phys. Lett. B **427** (1998) 85 [arXiv:hep-th/9802061].
- [9] S. Fredenhagen, M.R. Gaberdiel and C. Schmidt-Colinet, ‘Bulk flows in Virasoro minimal models with boundaries’, J. Phys. A **42** (2009) 495403 [arXiv:0907.2560 [hep-th]].
- [10] J.E. Bourguine, K. Hosomichi and I. Kostov, ‘Boundary transitions of the O(n) model on a dynamical lattice’, Nucl. Phys. B **832** (2010) 462 [arXiv:0910.1581 [hep-th]].
- [11] Al.B. Zamolodchikov, ‘Resonance factorized scattering and roaming trajectories’, J. Phys. A **39** (2006) 12847.
- [12] M.J. Martins, ‘Renormalization group trajectories from resonance factorized S matrices’, Phys. Rev. Lett. **69** (1992) 2461 [arXiv:hep-th/9205024].
- [13] P.E. Dorey and F. Ravanini, ‘Staircase models from affine Toda field theory’, Int. J. Mod. Phys. A **8** (1993) 873 [arXiv:hep-th/9206052].
- [14] M.J. Martins, ‘Analysis of asymptotic conditions in resonance functional hierarchies’, Phys. Lett. B **304** (1993) 111.
- [15] P. Dorey and F. Ravanini, ‘Generalizing the staircase models’, Nucl. Phys. B **406** (1993) 708 [arXiv:hep-th/9211115].
- [16] Al.B. Zamolodchikov, ‘From tricritical Ising to critical Ising by thermodynamic Bethe ansatz’, Nucl. Phys. B **358** (1991) 524.

- [17] A.B. Zamolodchikov, ‘Renormalization group and perturbation theory near fixed points in two-dimensional field theory’, *Sov. J. Nucl. Phys.* **46** (1987) 1090 [*Yad. Fiz.* **46** (1987) 1819].
  - [18] A.W.W. Ludwig and J.L. Cardy, ‘Perturbative evaluation of the conformal anomaly at new critical points with applications to random systems’, *Nucl. Phys. B* **285**, 687 (1987).
  - [19] M. Lassig, ‘Multiple crossover phenomena and scale hopping in two-dimensions’, *Nucl. Phys. B* **380** (1992) 601 [arXiv:hep-th/9112032].
  - [20] S. Ghoshal and A. B. Zamolodchikov, ‘Boundary S matrix and boundary state in two-dimensional integrable quantum field theory’, *Int. J. Mod. Phys. A* **9** (1994) 3841 [Erratum-ibid. *A* **9** (1994) 4353] [arXiv:hep-th/9306002].
  - [21] S. Ghoshal, ‘Bound state boundary S matrix of the sine-Gordon model’, *Int. J. Mod. Phys. A* **9** (1994) 4801 [arXiv:hep-th/9310188].
  - [22] E. Corrigan and G.W. Delius, ‘Boundary breathers in the sinh-Gordon model’, *J. Phys. A* **32** (1999) 8601 [arXiv:hep-th/9909145].
  - [23] P. Bowcock, E. Corrigan and C. Zambon, ‘Some aspects of jump-defects in the quantum sine-Gordon model’, *JHEP* **0508** (2005) 023 [arXiv:hep-th/0506169].
  - [24] Z. Bajnok and Zs. Simon, ‘Solving topological defects via fusion’, *Nucl. Phys. B* **802** (2008) 307 [arXiv:0712.4292 [hep-th]].
  - [25] J.L. Cardy, ‘Boundary conditions, fusion rules and the Verlinde formula’, *Nucl. Phys. B* **324** (1989) 581.
  - [26] A.B. Zamolodchikov, ‘Thermodynamic Bethe ansatz for RSOS scattering theories’, *Nucl. Phys. B* **358** (1991) 497.
  - [27] V.V. Bazhanov, S.L. Lukyanov and A.B. Zamolodchikov, ‘Quantum field theories in finite volume: Excited state energies’, *Nucl. Phys. B* **489** (1997) 487 [arXiv:hep-th/9607099].
  - [28] P. Dorey and R. Tateo, ‘Excited states by analytic continuation of TBA equations’, *Nucl. Phys. B* **482** (1996) 639 [arXiv:hep-th/9607167].
  - [29] K. Graham, ‘On perturbations of unitary minimal models by boundary condition changing operators’, *JHEP* **0203** (2002) 028 [arXiv:hep-th/0111205].
  - [30] C.R. Fernandez-Pousa, M.V. Gallas, T.J. Hollowood and J.L. Miramontes, ‘The symmetric space and homogeneous sine-Gordon theories’, *Nucl. Phys. B* **484** (1997) 609 [arXiv:hep-th/9606032].
  - [31] O.A. Castro-Alvaredo, A. Fring, C. Korff and J.L. Miramontes, ‘Thermodynamic Bethe ansatz of the homogeneous sine-Gordon models’, *Nucl. Phys. B* **575** (2000) 535 [arXiv:hep-th/9912196].
  - [32] P. Dorey and J.L. Miramontes, ‘Mass scales and crossover phenomena in the homogeneous sine-Gordon models’, *Nucl. Phys. B* **697** (2004) 405 [arXiv:hep-th/0405275].
-